Admissible Matrix Formulation :

from Orthogonal Approach to Explicit Hybrid Stabilization

K.Y.Sze

School of Mechanical & Production Engineering, Nanyang Technological University
Nanyang Avenue, SINGAPORE 2263

Abstract

Admissible Matrix Formulation is a patch test approach for efficient construction of multi-field finite element models. In hybrid stress and strain elements, the formulation employs the patch test patch to identify the constraints on, respectively, the flexibility and stiffness matrices which are most detrimental to the element efficiency. Admissible changes are introduced to the matrices so as to reduce the computational cost while the element accuracy remains virtually intact. In this paper, a comprehensive review of Admissible Matrix Formulation is presented. Finite element techniques seminal to the formulation are also discussed.

Published in ***Finite Elements in Analysis & Design,*** vol.24, 1-30 (1996)

Special Issue on **"Recent Development of Hybrid/Mixed Elements"**

1. Introduction

Since Pian's momentous paper on hybrid stress element formulation was published in 1964 [1], multi-field functionals have become one of the standard tools for designing and justifying advanced finite element models. In this paper, the definition of hybrid elements given by Pian in a recent keynote lecture is adopted, namely *hybrid elements are formulated by multi-field variational functionals, yet the only unknowns in the resulting global equation are still the nodal displacements* [2]. Owing to their multi-field nature which provides additional control over the element behaviour, hybrid elements have gained remarkable success in circumventing the deficiencies of the displacement elements. These deficiencies include membrane/shear locking, dilatational locking [3,4], susceptibility to mesh distortion, complications in constructing C^1 displacement profile for C^1 plate/shell models, poor performance in stress singularity and material discontinuity problems [5-7] etc. However, this nature also give rises to new problems such as frame invariance, nodal invariance (element symmetry) [8,9], optimal choice of the assumed stress/strain field, suppression of deformation modes and high computational cost in condensing the assumed stress/strain field. Only a few references are cited for the aforementioned issues as many of them would be addressed separately by other contributors of this special journal issue on hybrid/mixed elements.

Admissible Matrix Formulation (*AMF*) which has been established as a tool for reducing the computational cost of hybrid elements is expounded in this paper. For hybrid stress elements, *AMF* employs the patch test to identify the constraints on the flexibility matrix. Changes admissible to the identified constraints are introduced in the flexibility matrix to enhance the element efficiency. *AMF* was first applied to lower order elements with incompatible displacement modes. After realizing the computational burden incurred by the incompatible modes, *AMF* was then generalized to lower order elements with no incompatible modes. Difficulties were then encountered in extending *AMF* to higher order elements and a stabilization approach was adopted. In the approach, the leverage matrix pertinent to the assumed higher order stress modes plays the role of stabilizing the sub-integrated element. For some elements, if the assumed stress is strictly contravariant, the leverage matrix can be made very simple and formed explicitly in the element subroutine.

In the comprehensive account of the SemiLoof elements [10] (whose complexity can be significantly reduced by using the hybrid formulation [11,12]), the late Irons' wrote : *no formulation merges from a historical vacuum*. *AMF* is not an exception. Seminal ideas leading to *AMF* will be addressed. Among them, the orthogonal approach comes first.

2. Orthogonal Approach

Orthogonal Approach was first reported by Chen, Chow & Sze and submitted for reviewing in 1989 [13]. Unfortunately, substantial delay was encountered in the editorial process of the journal concerned. Since other papers by Chen & Cheung and Sze & Chow [14-17] rooted in the approach have been published elsewhere, withdrawal of reference [13] was decided. As a result, the manuscript has never been published.

The *Orthogonal Approach* starts with an extended elementwise Hu-Washizu functional [13,15,17] :

$$\Pi^{e}_{\sigma\varepsilon} = \left\langle \frac{1}{2}\boldsymbol{\varepsilon}^{T}\,\mathbf{C}\,\boldsymbol{\varepsilon} - \boldsymbol{\sigma}^{T}\,\mathbf{D}\mathbf{u}_{q} - \boldsymbol{\sigma}^{T}\,\mathbf{D}\mathbf{u}_{\lambda} \right\rangle - \int_{St} \mathbf{u}_{q}^{T}\,\mathbf{t}\,ds \qquad \text{where} \qquad \left\langle \mathbf{D}\mathbf{u}_{\lambda} \right\rangle = \mathbf{0} \quad (1)$$

in which $\boldsymbol{\varepsilon}$ is the assumed strain, $\mathbf{C}$ is the material stiffness matrix, $\boldsymbol{\sigma}$ is the assumed stress, $\mathbf{D}$ is the strain-displacement operator, $\langle\ \rangle$ denotes the integration over the element domain and $\mathbf{t}$ is the prescribed traction applied over the portion of element boundary denoted by *St*. Displacements $\mathbf{u}_q$ and $\mathbf{u}_\lambda$ are compatible and incompatible, respectively. Throughout this paper, the material properties are assumed to be constant inside an element. Without sacrificng generality, the assumed stress and strain can be partitioned into constant "c" and non-constant "n" modes :

$$\boldsymbol{\sigma} = \boldsymbol{\sigma}_c + \boldsymbol{\sigma}_n = \boldsymbol{\beta}_c + \mathbf{P}_n\,\boldsymbol{\beta}_n = \begin{bmatrix} \mathbf{I}_c & \mathbf{P}_n \end{bmatrix} \begin{Bmatrix} \boldsymbol{\beta}_c \\ \boldsymbol{\beta}_n \end{Bmatrix} \quad , \qquad \boldsymbol{\varepsilon} = \boldsymbol{\varepsilon}_c + \boldsymbol{\varepsilon}_n = \boldsymbol{\alpha}_c + \mathbf{Q}_n\,\boldsymbol{\alpha}_n = \begin{bmatrix} \mathbf{I}_c & \mathbf{Q}_n \end{bmatrix} \begin{Bmatrix} \boldsymbol{\alpha}_c \\ \boldsymbol{\alpha}_n \end{Bmatrix}$$

(2a,b)

and the discretized displacements are written as :

$$\mathbf{u}_q = \mathbf{N}_q\,\mathbf{q} \quad , \quad \mathbf{u}_\lambda = \mathbf{N}_\lambda\,\boldsymbol{\lambda} \qquad (3a,b)$$

where $\mathbf{I}_c$ is the identity matrix of order equal to dim.($\boldsymbol{\varepsilon}$), $\mathbf{q}$ is the nodal displacement vector, $\boldsymbol{\alpha}$'s, $\boldsymbol{\beta}$'s and $\boldsymbol{\lambda}$ are vectors of coefficients to be condensed in the element level. For $\left\langle \mathbf{D}\mathbf{u}_\lambda \right\rangle$ not equal to zero, $\boldsymbol{\sigma}^T\mathbf{D}\mathbf{u}_\lambda$ in Eqn.(1) should be replaced by $\boldsymbol{\sigma}_n^T\mathbf{D}\mathbf{u}_\lambda$. The assumed non-constant stress and strain shape function matrices are often chosen to have the following uncoupled structure :

$$\mathbf{P}_n = \begin{bmatrix} \mathbf{I}_c f_1 & \mathbf{I}_c f_2 & \cdots & \mathbf{I}_c f_m \end{bmatrix} \quad , \quad \mathbf{Q}_n = \frac{1}{J}\begin{bmatrix} \mathbf{I}_c f_1 & \mathbf{I}_c f_2 & \cdots & \mathbf{I}_c f_m \end{bmatrix}$$

(4a,b)

where J is the Jacobian determinant, f_i's are simple polynomial terms of the natural coordinates (ξ,η,ζ). The above choices of stress and strain are advantageous in simplifying some matrix operations and probably inherent from the early works of Pian and his coworkers [18-20], Chen & Cheung [21,22]. Moreover,

$$\left\langle f_i / J \right\rangle = \int_{-1}^{+1}\int_{-1}^{+1}\int_{-1}^{+1} f_i\,d\xi d\eta d\zeta = 0 \qquad \text{for all } i\text{'s}, \quad \text{i.e.} \qquad \left\langle \mathbf{Q}_n \right\rangle = \mathbf{0}$$

(5a)

$$\int_{-1}^{+1}\int_{-1}^{+1}\int_{-1}^{+1} f_i\, f_j\, d\xi d\eta d\zeta = \bar{f}_i\, \delta_{ij} = \bar{f}_j \delta_{ij} \tag{5b}$$

in which δ_{ij} is the Kronecker delta. Substitutions of Eqn.(2), Eqn.(3), Eqn.(4) and Eqn.(5) into Eqn.(1) result in :

$$\begin{aligned}\Pi^e_{\sigma\varepsilon} = \frac{1}{2}\begin{Bmatrix}\boldsymbol{\alpha}_c\\ \boldsymbol{\alpha}_n\end{Bmatrix}^T\begin{bmatrix} v\mathbf{C} & \mathbf{0}\\ \mathbf{0} & \left\langle \mathbf{Q}_n^T\mathbf{C}\mathbf{Q}_n\right\rangle\end{bmatrix}\begin{Bmatrix}\boldsymbol{\alpha}_c\\ \boldsymbol{\alpha}_n\end{Bmatrix} - \begin{Bmatrix}\boldsymbol{\beta}_c\\ \boldsymbol{\beta}_n\end{Bmatrix}^T\begin{bmatrix} v\mathbf{I}_c & \mathbf{0}\\ \left\langle \mathbf{P}_n^T\right\rangle & \left\langle \mathbf{P}_n^T\mathbf{Q}_n\right\rangle\end{bmatrix}\begin{Bmatrix}\boldsymbol{\alpha}_c\\ \boldsymbol{\alpha}_n\end{Bmatrix}\\ + \begin{Bmatrix}\boldsymbol{\beta}_c\\ \boldsymbol{\beta}_n\end{Bmatrix}^T\begin{bmatrix} \left\langle \mathbf{D}\mathbf{N}_q\right\rangle & \left\langle \mathbf{D}\mathbf{N}_\lambda\right\rangle\\ \left\langle \mathbf{P}_n^T\mathbf{D}\mathbf{N}_q\right\rangle & \left\langle \mathbf{P}_n^T\mathbf{D}\mathbf{N}_\lambda\right\rangle\end{bmatrix}\begin{Bmatrix}\mathbf{q}\\ \boldsymbol{\lambda}\end{Bmatrix} - \mathbf{q}^T\int_{St}\mathbf{N}_q^T\mathbf{t}\,ds\end{aligned} \tag{6}$$

If the Jacobian determinant is replaced by its mean in evaluating the stiffness matrix $\left\langle \mathbf{Q}_n^T\mathbf{C}\mathbf{Q}_n\right\rangle$, i.e.

$$J \;\rightarrow\; \bar{J} = v \Big/ \int_{-1}^{+1}\int_{-1}^{+1}\int_{-1}^{+1} d\xi d\eta d\zeta \quad \text{and} \quad v = \langle 1\rangle = \int_{-1}^{+1}\int_{-1}^{+1}\int_{-1}^{+1} J(\xi,\eta,\zeta)\, d\xi d\eta d\zeta \tag{7a,b}$$

where "$\rightarrow$" denotes "is changed to", the matrix becomes :

$$\mathbf{M}_n = \frac{1}{\bar{J}}\int_{-1}^{+1}\int_{-1}^{+1}\int_{-1}^{+1}\mathbf{P}_n^T\mathbf{C}\mathbf{P}_n\; d\xi d\eta d\zeta = \frac{1}{\bar{J}}\cdot \text{diag.}\left\{\bar{f}_1\mathbf{C} \quad \cdots \quad \bar{f}_m\mathbf{C}\right\} \tag{8}$$

After replacing $\left\langle \mathbf{Q}_n^T\mathbf{C}\mathbf{Q}_n\right\rangle$ by $\mathbf{M}_n$, the functional becomes :

$$\begin{aligned}\Pi^e_{\sigma\varepsilon} = \frac{1}{2}\begin{Bmatrix}\boldsymbol{\alpha}_c\\ \boldsymbol{\alpha}_n\end{Bmatrix}^T\begin{bmatrix} v\mathbf{C} & \mathbf{0}\\ \mathbf{0} & \mathbf{M}_n\end{bmatrix}\begin{Bmatrix}\boldsymbol{\alpha}_c\\ \boldsymbol{\alpha}_n\end{Bmatrix} - \begin{Bmatrix}\boldsymbol{\beta}_c\\ \boldsymbol{\beta}_n\end{Bmatrix}^T\begin{bmatrix} v\mathbf{I}_c & \mathbf{0}\\ \left\langle \mathbf{P}_n^T\right\rangle & \left\langle \mathbf{P}_n^T\mathbf{Q}_n\right\rangle\end{bmatrix}\begin{Bmatrix}\boldsymbol{\alpha}_c\\ \boldsymbol{\alpha}_n\end{Bmatrix}\\ + \begin{Bmatrix}\boldsymbol{\beta}_c\\ \boldsymbol{\beta}_n\end{Bmatrix}^T\begin{bmatrix} \left\langle \mathbf{D}\mathbf{N}_q\right\rangle & \mathbf{0}\\ \left\langle \mathbf{P}_n^T\mathbf{D}\mathbf{N}_q\right\rangle & \left\langle \mathbf{P}_n^T\mathbf{D}\mathbf{N}_\lambda\right\rangle\end{bmatrix}\begin{Bmatrix}\mathbf{q}\\ \boldsymbol{\lambda}\end{Bmatrix} - \mathbf{q}^T\int_{St}\mathbf{N}_q^T\mathbf{t}\,ds\end{aligned}$$

(9)

Noting that

$$\begin{bmatrix} v\mathbf{I}_c & \mathbf{0}\\ \left\langle \mathbf{P}_n^T\right\rangle & \left\langle \mathbf{P}_n^T\mathbf{Q}_n\right\rangle\end{bmatrix}^{-1} = \begin{bmatrix} (1/v)\mathbf{I}_c & \mathbf{0}\\ -(1/v)\left\langle \mathbf{P}_n^T\mathbf{Q}_n\right\rangle^{-1}\left\langle \mathbf{P}_n^T\right\rangle & \left\langle \mathbf{P}_n^T\mathbf{Q}_n\right\rangle^{-1}\end{bmatrix} \tag{10a}$$

$$\left\langle \mathbf{P}_n^T \mathbf{DN}_q \right\rangle = \begin{bmatrix} \left\langle f_1 \mathbf{DN}_q \right\rangle \\ \vdots \\ \left\langle f_m \mathbf{DN}_q \right\rangle \end{bmatrix} \quad , \quad \left\langle \mathbf{P}_n^T \mathbf{DN}_q \right\rangle = \begin{bmatrix} \left\langle f_1 \mathbf{DN}_\lambda \right\rangle \\ \vdots \\ \left\langle f_m \mathbf{DN}_\lambda \right\rangle \end{bmatrix} \quad , \quad \left\langle \mathbf{P}_n^T \right\rangle = \begin{bmatrix} \left\langle f_1 \right\rangle \mathbf{I}_c \\ \vdots \\ \left\langle f_m \right\rangle \mathbf{I}_c \end{bmatrix}$$

(10b,c,d)

$$\left\langle \mathbf{P}_n^T \mathbf{Q}_n \right\rangle^{-1} = \text{diag.} \left\{ \frac{1}{\bar{f}_1} \mathbf{I}_c \qquad \frac{1}{\bar{f}_m} \mathbf{I}_c \right\} \quad , \quad \left\langle \mathbf{P}_n^T \mathbf{Q}_n \right\rangle^{-1} \left\langle \mathbf{P}_n^T \right\rangle = \begin{bmatrix} \frac{\left\langle f_1 \right\rangle}{\bar{f}_1} \mathbf{I}_c & \cdots & \frac{\left\langle f_m \right\rangle}{\bar{f}_m} \mathbf{I}_c \end{bmatrix}^T \quad (10e)$$

variations of $\boldsymbol{\alpha}$'s and $\boldsymbol{\beta}$'s in the functional enforce :-

$$\begin{Bmatrix} \boldsymbol{\alpha}_c \\ \boldsymbol{\alpha}_n \end{Bmatrix} = \begin{bmatrix} v\mathbf{I}_c & \mathbf{0} \\ \left\langle \mathbf{P}_n^T \right\rangle & \left\langle \mathbf{P}_n^T \mathbf{Q}_n \right\rangle \end{bmatrix}^{-1} \begin{bmatrix} \left\langle \mathbf{DN}_q \right\rangle & \mathbf{0} \\ \left\langle \mathbf{P}_n^T \mathbf{DN}_q \right\rangle & \left\langle \mathbf{P}_n^T \mathbf{DN}_\lambda \right\rangle \end{bmatrix} \begin{Bmatrix} \mathbf{q} \\ \boldsymbol{\lambda} \end{Bmatrix} = \begin{bmatrix} \frac{1}{v} \left\langle \mathbf{DN}_q \right\rangle & \mathbf{0} \\ \mathbf{B}_{q1} & \mathbf{B}_{\lambda 1} \\ \vdots & \vdots \\ \mathbf{B}_{qm} & \mathbf{B}_{\lambda m} \end{bmatrix} \begin{Bmatrix} \mathbf{q} \\ \boldsymbol{\lambda} \end{Bmatrix}$$

(11a)

and

$$\begin{Bmatrix} \boldsymbol{\beta}_c \\ \boldsymbol{\beta}_n \end{Bmatrix} = \begin{bmatrix} v\mathbf{I}_c & \mathbf{0} \\ \left\langle \mathbf{P}_n^T \right\rangle & \left\langle \mathbf{P}_n^T \mathbf{Q}_n \right\rangle \end{bmatrix}^{-T} \begin{bmatrix} v\mathbf{C} & \mathbf{0} \\ \mathbf{0} & \mathbf{M}_n \end{bmatrix} = \begin{bmatrix} \mathbf{C} & & \mathbf{0} \\ \begin{bmatrix} \frac{-\left\langle f_1 \right\rangle}{\bar{f}_1} \mathbf{C} & \cdots & \frac{-\left\langle f_m \right\rangle}{\bar{f}_m} \mathbf{C} \end{bmatrix}^T & & \frac{1}{\bar{J}} \cdot diag. \begin{Bmatrix} \mathbf{C} & \cdots & \mathbf{C} \end{Bmatrix} \end{bmatrix} \begin{Bmatrix} \boldsymbol{\alpha}_c \\ \boldsymbol{\alpha}_n \end{Bmatrix}$$

(11b)

where

$$\mathbf{B}_{qi} = \frac{1}{\bar{f}_i} \left\langle f_i \mathbf{DN}_q \right\rangle - \frac{\left\langle f_i \right\rangle}{v \bar{f}_i} \left\langle \mathbf{DN}_q \right\rangle \qquad \text{and} \qquad \mathbf{B}_{\lambda i} = \frac{1}{\bar{f}_i} \left\langle f_i \mathbf{DN}_\lambda \right\rangle$$

After condensing $\boldsymbol{\beta}$'s and $\boldsymbol{\alpha}$'s,

$$\Pi_{\sigma\varepsilon}^e = \frac{1}{2} \begin{Bmatrix} \mathbf{q} \\ \boldsymbol{\lambda} \end{Bmatrix}^T \left(\frac{1}{v} \begin{bmatrix} \left\langle \mathbf{DN}_q \right\rangle^T \mathbf{C} \left\langle \mathbf{DN}_q \right\rangle & \mathbf{0} \\ \mathbf{0} & \mathbf{0} \end{bmatrix} + \sum_{i=1}^{m} \frac{\bar{f}_i}{\bar{J}} [\mathbf{B}_{qi} \quad \mathbf{B}_{\lambda i}]^T \mathbf{C} [\mathbf{B}_{qi} \quad \mathbf{B}_{\lambda i}] \right) \begin{Bmatrix} \mathbf{q} \\ \boldsymbol{\lambda} \end{Bmatrix} - \mathbf{q}^T \int_{St} \mathbf{N}_q^T \mathbf{t} \, ds \quad (12)$$

Hence, the generalized element stiffness matrix (inside the parenthesis) is the sum of a series. The element stiffness matrix can be obtained by condensing $\boldsymbol{\lambda}$. The attraction of the orthogonal approach as compared to the conventional hybrid formulation is attributed to the block-diagonal nature of $\left\langle \mathbf{P}_n^T \mathbf{Q}_n \right\rangle$ and $\mathbf{M}_n$.

At the time reference [13] was completed, it was not understood : (Q1) why changing $\left\langle \mathbf{Q}_n^T \mathbf{C} \mathbf{Q}_n \right\rangle$ to $\mathbf{M}_n$ does not lead to patch test failure; (Q2) if the orthogonality between the constant and non-constant assumed strain modes does not hold, i.e. $\left\langle \mathbf{Q}_n \right\rangle \neq \mathbf{0}$, why the resulting element fails the patch test after

$$\left\langle \begin{bmatrix} \mathbf{I}_c & \mathbf{Q}_n \end{bmatrix}^T \mathbf{C} \begin{bmatrix} \mathbf{I}_c & \mathbf{Q}_n \end{bmatrix} \right\rangle = \begin{bmatrix} v\mathbf{C} & \mathbf{C}\left\langle \mathbf{Q}_n \right\rangle \\ \text{sym.} & \left\langle \mathbf{Q}_n^T \mathbf{C} \mathbf{Q}_n \right\rangle \end{bmatrix} \quad \rightarrow \quad \begin{bmatrix} v\mathbf{C} & \mathbf{0} \\ \mathbf{0} & \mathbf{M}_n \end{bmatrix} \tag{13}$$

(Q3) whether the same philosophy can be applied to elements based on the simpler Hellinger-Reissner functional and its extensions.

3. Patch Test : a Tool for Designing Finite Element Models

The inspiration for answering (Q1) and (Q2) came from Bergan & Hanssen's work of using the i*ndividual element test* to design finite element models [23]. By using this special form of patch test, linear constraints on the stiffness matrix of the assumed displacement element are identified. These constraints serve as the clue in designing the nodal displacement interpolants which need not be pointwisely compatible and form the foundation for *free formulation* [24,25].

With the notion of designing finite element models by patch test in mind, the author & Chow employed the *form C test* (also known as the generalized patch test) to examine the admissible changes in the flexibility and stiffness matrices of, respectively, the hybrid stress and strain elements [14,16]. For an element assemblage, the *form C test* is performed by *fixing the minimal number of nodal displacement d.o.f.s (for suppression of the rigid body motions) and prescribing the natural boundary conditions at the remaining boundary d.o.f.s in accordance with an arbitrary constant stress/strain state. The test is satisfied if the predicted stress/strain, displacement and nodal forces are all exact* [26]. To ensure the element stability, the *one element form C test* should also be considered. In contrast to the *individual element test*, the *one element form C test* can validate the element stability but not the pairwise cancellation of traction. Recently, Militello & Felippa proved that *individual element test* together with the element stability would secure the fulfillment of the *form C test* [27].

Let $\hat{\mathbf{u}}$ represent an arbitrary displacement field such that the derived strain $\mathbf{D}\hat{\mathbf{u}} = \hat{\boldsymbol{\varepsilon}}$ is a constant (including zero) and $\hat{\mathbf{q}}$ be the element nodal displacement vector obtained by collocating the nodal displacements with $\hat{\mathbf{u}}$. Moreover, the element boundary displacement interpolation is denoted as :

$$\mathbf{v} = \boldsymbol{\Gamma}\, \mathbf{q} \tag{14}$$

where $\boldsymbol{\Gamma}$ is the interpolation matrix. For an element model with stiffness $\mathbf{K}$, the requirements of the *individual element test* [23,24,27], *form A*, *form B* and *form C patch tests* [26], see Fig.1, can be consolidated into :

(C1) essential boundary condition (e.b.c.) consistency :

when $\hat{\mathbf{q}}$ is prescribed, all the computed stresses and strains are exact

(C2) natural boundary condition (n.b.c.) consistency :

$\mathbf{K}\hat{\mathbf{q}} = \oint \boldsymbol{\Gamma}^T \mathbf{n}\, ds\, \mathbf{C}\hat{\boldsymbol{\varepsilon}}$ where $\oint ds$ denotes the closed boundary integration of the element and $\mathbf{n}$ is the traction-stress matrix.

(C3) weak form of displacement compatibility :

$\int_{S_{com}} \mathbf{n}_a^T \mathbf{v}_a\, ds = \int_{S_{com}} \mathbf{n}_b^T \mathbf{v}_b\, ds$ or $\int_{S_{com}} \mathbf{n}_a^T \boldsymbol{\Gamma}_a\, ds\, \mathbf{q}_a = \int_{S_{com}} \mathbf{n}_b^T \boldsymbol{\Gamma}_b\, ds\, \mathbf{q}_b$

for any pair of adjacent elements "a" and "b" where S_{com} is their common boundary (note : $\mathbf{n}_a = -\mathbf{n}_b$).

(C4) stability :

besides the rigid body modes, the element does not possess any zero energy mode.

(C1) leads directly to the fulfillment of *form A test*. For the two adjacent elements under the same constant stress, (C3) immediately implies the pairwise cancellation of traction [23,24,27]. Thus, (C3) leads to the fulfillment of *form B test* whereas (C2) and (C3) lead to the fulfillment of the *individual element test*. Finally, (C2) and (C4) leads to the fulfillment of the *one element form C test*.

In an element assemblage containing more than one element and at least one internal nodes, when the global displacement vector $\mathbf{q}_G$ is set to $\hat{\mathbf{q}}_G$ which is obtained by collocating $\mathbf{q}_G$ with $\hat{\mathbf{u}}$, we have

$$\begin{aligned}\delta\mathbf{q}_G^T \mathbf{K}_G \hat{\mathbf{q}}_G &= \sum_e \delta\mathbf{q}^T \mathbf{K}\hat{\mathbf{q}} = \sum_e \delta\mathbf{q}^T \oint \boldsymbol{\Gamma}^T \mathbf{n}\, ds\, \mathbf{C}\hat{\boldsymbol{\varepsilon}} \\ &= \sum_e \delta\mathbf{q}^T \int_{S_{com}} \boldsymbol{\Gamma}^T \mathbf{n}\, ds\, \mathbf{C}\hat{\boldsymbol{\varepsilon}} + \sum_e \delta\mathbf{q}^T \int_{S_{ext}} \boldsymbol{\Gamma}^T \mathbf{n}\, ds\, \mathbf{C}\hat{\boldsymbol{\varepsilon}} = \sum_e \delta\mathbf{q}^T \int_{S_{ext}} \boldsymbol{\Gamma}^T \mathbf{n}\, ds\, \mathbf{C}\hat{\boldsymbol{\varepsilon}}\end{aligned}$$

(15)

where $\mathbf{K}_G$ is the global matrix, $\sum_e$ denotes the summation over all the elements and S_{ext} denotes the portions of element boundary common to the boundary of the assemblage. In the manipulation of Eqn.(15), (C2) and (C3) have been incorporated. It can be seen that the global nodal force vectors resulting from mulitiplying $\mathbf{K}_G$ with $\hat{\mathbf{q}}_G$ and assembling the boundary integrals over S_{ext}'s (note : all S_{ext}'s constitute the entire boundary of the assemblage) are identical. In other words,

n.b.c consistency also holds for the assemblage. If the assemblage has been restrained from all rigid body modes, the n.b.c. consistency of the assemblage and (C4) ensure that $\hat{\mathbf{q}}_G$ is the unique solution of the restrained assemblage. Therefore, the element model also passes the *form C test*.

4. Patch Test Approach for Designing Displacement-Based Elements

Taking the displacement-based element as an example for the patch test approach of element design, the element strains are expressed as :

$$\boldsymbol{\varepsilon}^u = \boldsymbol{\varepsilon}_q + \boldsymbol{\varepsilon}_\lambda \quad , \quad \boldsymbol{\varepsilon}_q = \mathbf{B}_q\,\mathbf{q} \quad , \quad \boldsymbol{\varepsilon}_\lambda = \mathbf{B}_\lambda\,\boldsymbol{\lambda}$$

(16a,b,c)

It should be remarked that $\mathbf{B}_q$ and $\mathbf{B}_\lambda$ are not necessarily equal to $\mathbf{D}$ operated on some displacement interpolation matrices. This allows us to include the assumed strain, B-bar, enhanced strain methods, etc [28-32]. The functional used to formulate the element is :

$$\Pi^e = \frac{1}{2}\begin{Bmatrix}\mathbf{q}\\ \boldsymbol{\lambda}\end{Bmatrix}^T\begin{bmatrix}\left\langle \mathbf{B}_q^T\mathbf{C}\mathbf{B}_q\right\rangle & \left\langle \mathbf{B}_q^T\mathbf{C}\mathbf{B}_\lambda\right\rangle\\ \textit{sym.} & \left\langle \mathbf{B}_\lambda^T\mathbf{C}\mathbf{B}_\lambda\right\rangle\end{bmatrix}\begin{Bmatrix}\mathbf{q}\\ \boldsymbol{\lambda}\end{Bmatrix} - \mathbf{q}^T\int_{St}\boldsymbol{\Gamma}^T\,\mathbf{t}\,ds \tag{17}$$

$\boldsymbol{\lambda}$ is the vector of internal d.o.f.s (bubble displacements, incompatible displacements and enhance strain modes) and will be condensed in the element level. Hence, n.b.c. cannot be prescribed via $\boldsymbol{\lambda}$ and the conjugate force of $\boldsymbol{\lambda}$ must be zero as noted in the equation. Variation of $\boldsymbol{\lambda}$ enforces :

$$\left\langle \mathbf{B}_\lambda^T\mathbf{C}\mathbf{B}_q\right\rangle\mathbf{q} + \left\langle \mathbf{B}_\lambda^T\mathbf{C}\mathbf{B}_\lambda\right\rangle\boldsymbol{\lambda} = \left\langle \mathbf{B}_\lambda^T\mathbf{C}\boldsymbol{\varepsilon}^u\right\rangle = \mathbf{0} \tag{18}$$

After condensing $\boldsymbol{\lambda}$,

$$\Pi^e = \frac{1}{2}\mathbf{q}^T\left(\left\langle \mathbf{B}_q^T\mathbf{C}\mathbf{B}_q\right\rangle - \left\langle \mathbf{B}_q^T\mathbf{C}\mathbf{B}_\lambda\right\rangle\left\langle \mathbf{B}_\lambda^T\mathbf{C}\mathbf{B}_\lambda\right\rangle^{-1}\left\langle \mathbf{B}_\lambda^T\mathbf{C}\mathbf{B}_q\right\rangle\right)\mathbf{q} - \mathbf{q}^T\int_{St}\boldsymbol{\Gamma}^T\,\mathbf{t}\,ds \tag{19}$$

Consideration for (C1) : It is assumed that $\hat{\boldsymbol{\varepsilon}} \in \boldsymbol{\varepsilon}^u$ for any constant strain $\hat{\boldsymbol{\varepsilon}}$. In other words, we can always find $\hat{\mathbf{q}}$ and $\hat{\boldsymbol{\lambda}}$ such that

$$\boldsymbol{\varepsilon}^u = \mathbf{B}_q\,\hat{\mathbf{q}} + \mathbf{B}_\lambda\,\hat{\boldsymbol{\lambda}} = \hat{\boldsymbol{\varepsilon}} \tag{20}$$

For the consistency of Eqn.(18) and owing to the arbitrary nature of $\hat{\boldsymbol{\varepsilon}}$,

$$\left\langle \mathbf{B}_\lambda^T\right\rangle\mathbf{C}\hat{\boldsymbol{\varepsilon}} = \mathbf{0} \quad \text{or} \quad \left\langle \mathbf{B}_\lambda\right\rangle = \mathbf{0} \tag{21a,b}$$

This is the well-known consistency criterion for incompatible internal d.o.f.s and the enhanced strain modes [32,33].

Consideration for (C2) : For the validity of (C2) and by recalling Eqn.(18), Eqn.(19) and Eqn.(20), we should have

$$\oint \mathbf{\Gamma}^T \mathbf{n}\, ds\ \mathbf{C}\hat{\boldsymbol{\varepsilon}} = \left(\left\langle \mathbf{B}_q^T \mathbf{C} \mathbf{B}_q \right\rangle - \left\langle \mathbf{B}_q^T \mathbf{C} \mathbf{B}_\lambda \right\rangle \left\langle \mathbf{B}_\lambda^T \mathbf{C} \mathbf{B}_\lambda \right\rangle^{-1} \left\langle \mathbf{B}_\lambda^T \mathbf{C} \mathbf{B}_q \right\rangle \right) \hat{\mathbf{q}}$$

$$= \left\langle \mathbf{B}_q^T \mathbf{C} \mathbf{B}_q \right\rangle \hat{\mathbf{q}} + \left\langle \mathbf{B}_q^T \mathbf{C} \mathbf{B}_\lambda \right\rangle \hat{\boldsymbol{\lambda}} = \left\langle \mathbf{B}_q^T \right\rangle \mathbf{C}\hat{\boldsymbol{\varepsilon}} \qquad (22a)$$

or

$$\oint \mathbf{\Gamma}^T \mathbf{n}\, ds = \left\langle \mathbf{B}_q^T \right\rangle \qquad (22b)$$

The condition always hold if $\mathbf{B}_q$ is derived from a displacement interpolation matrix, i.e. $\mathbf{B}_q = \mathbf{D}\mathbf{N}_q$, and $\mathbf{\Gamma}$ equals $\mathbf{N}_q$ over the element boundary as a result of the divergence theorem.

Consideration for (C3) : Being a compatibility condition, (C3) depends purely on the choice of $\mathbf{\Gamma}$. Since $\int_{Sc} \mathbf{n}_a^T \mathbf{\Gamma}_a\, ds\ \mathbf{q}_a = \int_{Sc} \mathbf{n}_b^T \mathbf{\Gamma}_b\, ds\ \mathbf{q}_b$ is rather apparent, no further deduction will be attempted.

Consideration for (C4) : If $\boldsymbol{\varepsilon}^u$ has the proper kernal (i.e. $\boldsymbol{\varepsilon}^u$ vanishes only for the rigid body modes) and the strain energy is fully integrated, (C4) will be valid as $\mathbf{C}$ is positive definite. Full or standard order of integration is defined as the least order of quadrature that can exactly evaluate the highest order polynomial term in an integral when the element is regular in geometry. If the integral is computed by using a lower order quadrature, it is said to be sub-integrated.

In particular, *free formulation* is commonly perceived as a methodology for designing a special kind of incompatible displacement-based elements which are different from the more popular λ-type incompatible elements [34-36]. In the simplest sense, *free formulated* elements employ :

$$\mathbf{B}_q = \mathbf{D}\mathbf{N}_q \qquad \text{and} \qquad \mathbf{\Gamma} = \mathbf{N}_q \qquad (23a,b)$$

However, the displacement interpolation only satisfies (C3) and is not pointwise compatible. Bergan, Felippa and their coworkers have derived a number of lower order plate/shell elements based on the *free formulation* and its extensions [23-25,37,38].

5. AMF : The Patch Test Approach for Designing Hybrid Stress Elements

When *AMF* was first developed, it was termed *free formulation* as the former also employs the patch test to justify the admissible changes in the flexibility matrices [14]. Indeed, the original title of reference [16] was "Efficient hybrid/mixed elements using free formulation". The reviewer of the paper commented on the theoretical foundation and hybrid displacement nature of the *free formulation* [25] as opposed to *AMF* which employs a considerably different philosophy. Hence, the paper was renamed as "Efficient hybrid/mixed elements using admissible matrix formulation". In a Chicago conference back to 1991, the author submitted an abstract entitled " Derivation of accuracy and efficient elements by mixed method and free formulation" [39]. During the presentation, *AMF* was used in lieu of *free formulation*. It may be interesting to point out that Professor P.G.Bergan raised the question after the presentation on why *free formulation* was changed to *AMF*.

Consider the following elementwise extended Hellinger-Reissner functional in which $\boldsymbol{\sigma}$, $\boldsymbol{\varepsilon}^u$ and $\mathbf{v}$ have been given in Eqn.(2b), Eqn.(16) and Eqn.(14) :

$$\Pi_\sigma^e = -\frac{1}{2}\left\langle \boldsymbol{\sigma}^T \mathbf{S}\boldsymbol{\sigma} \right\rangle + \left\langle \boldsymbol{\sigma}^T \boldsymbol{\varepsilon}^u \right\rangle - \int_{St} \mathbf{v}^T \mathbf{t}\, ds \tag{24a}$$

or

$$\Pi_\sigma^e = -\frac{1}{2}\boldsymbol{\beta}^T \begin{bmatrix} v\mathbf{S} & \mathbf{S}\left\langle \mathbf{P}_n \right\rangle \\ sym. & \left\langle \mathbf{P}_n^T \mathbf{S} \mathbf{P}_n \right\rangle \end{bmatrix} \boldsymbol{\beta} + \boldsymbol{\beta}^T \begin{bmatrix} \mathbf{G}_q & \mathbf{G}_\lambda \end{bmatrix} \begin{Bmatrix} \mathbf{q} \\ \boldsymbol{\lambda} \end{Bmatrix} - \mathbf{q}^T \int_{St} \boldsymbol{\Gamma}^T \mathbf{t}\, ds \tag{24b}$$

where

$$\boldsymbol{\beta} = \begin{Bmatrix} \boldsymbol{\beta}_c \\ \boldsymbol{\beta}_n \end{Bmatrix} \quad , \mathbf{S} = \mathbf{C}^{-1} \quad \text{is the material compliance matrix}$$

After the following replacement :

$$\begin{bmatrix} v\mathbf{S} & \mathbf{S}\left\langle \mathbf{P}_n \right\rangle \\ sym. & \left\langle \mathbf{P}_n^T \mathbf{S} \mathbf{P}_n \right\rangle \end{bmatrix} \rightarrow \mathbf{H} = \begin{bmatrix} \mathbf{H}_{cc} & \mathbf{H}_{cn} \\ sym. & \mathbf{H}_{nn} \end{bmatrix} \tag{25}$$

we have

$$\Pi_\sigma^e = -\frac{1}{2}\boldsymbol{\beta}^T \mathbf{H} \boldsymbol{\beta} + \boldsymbol{\beta}^T \begin{bmatrix} \mathbf{G}_q & \mathbf{G}_\lambda \end{bmatrix} \begin{Bmatrix} \mathbf{q} \\ \boldsymbol{\lambda} \end{Bmatrix} - \mathbf{q}^T \int_{St} \boldsymbol{\Gamma}^T \mathbf{t}\, ds \tag{26}$$

Following the standard variational procedure,

$$\mathbf{H}\boldsymbol{\beta} = \mathbf{G}_q \mathbf{q} + \mathbf{G}_\lambda \boldsymbol{\lambda} \quad , \qquad \mathbf{G}_\lambda^T \boldsymbol{\beta} = \left\langle \mathbf{B}_\lambda \right\rangle^T \boldsymbol{\beta}_c + \left\langle \mathbf{P}_n^T \mathbf{B}_\lambda \right\rangle^T \boldsymbol{\beta}_n = \mathbf{0} \ , \qquad \mathbf{G}_\lambda^T \mathbf{H}^{-1} (\mathbf{G}_q \mathbf{q} + \mathbf{G}_\lambda \boldsymbol{\lambda}) = \mathbf{0}$$

(27a,b,c)

$$\Pi_{\sigma}^{e} = \frac{1}{2}\begin{Bmatrix}\mathbf{q}\\ \boldsymbol{\lambda}\end{Bmatrix}^{T}\begin{bmatrix}\mathbf{G}_q & \mathbf{G}_\lambda\end{bmatrix}^{T}\mathbf{H}^{-1}\begin{bmatrix}\mathbf{G}_q & \mathbf{G}_\lambda\end{bmatrix}\begin{Bmatrix}\mathbf{q}\\ \boldsymbol{\lambda}\end{Bmatrix} - \mathbf{q}^{T}\int_{St}\boldsymbol{\Gamma}^{T}\,\mathbf{t}\,ds$$

$$= \frac{1}{2}\mathbf{q}^{T}\left(\mathbf{G}_q^{T}\mathbf{H}^{-1}\mathbf{G}_q - \mathbf{G}_q^{T}\mathbf{H}^{-1}\mathbf{G}_\lambda(\mathbf{G}_\lambda^{T}\mathbf{H}^{-1}\mathbf{G}_\lambda)^{-1}\mathbf{G}_\lambda^{T}\mathbf{H}^{-1}\mathbf{G}_q\right)\mathbf{q} - \mathbf{q}^{T}\int_{St}\boldsymbol{\Gamma}^{T}\,\mathbf{t}\,ds$$

(27d)

Consideration for (C1) : Same as last section, existence of $\hat{\mathbf{q}}$ and $\hat{\boldsymbol{\lambda}}$ is assumed such that Eqn.(20) is valid. (C1) requires that $\boldsymbol{\beta}_c = \mathbf{C}\hat{\boldsymbol{\varepsilon}}$ and $\boldsymbol{\beta}_n = \mathbf{0}$ for $\boldsymbol{\varepsilon}^{u} = \mathbf{B}_q\hat{\mathbf{q}} + \mathbf{B}_\lambda\hat{\boldsymbol{\lambda}} = \hat{\boldsymbol{\varepsilon}}$. From Eqn.(27a) and Eqn.(27b),

$$\begin{bmatrix}\mathbf{H}_{cc} & \mathbf{H}_{cn}\\ sym. & \mathbf{H}_{nn}\end{bmatrix}\begin{Bmatrix}\mathbf{C}\hat{\boldsymbol{\varepsilon}}\\ \mathbf{0}\end{Bmatrix} = \mathbf{G}_q\hat{\mathbf{q}} + \mathbf{G}_\lambda\hat{\boldsymbol{\lambda}} = \left\langle\begin{bmatrix}\mathbf{I}_c\\ \mathbf{P}_n^{T}\end{bmatrix}(\mathbf{B}_q\hat{\mathbf{q}} + \mathbf{B}_\lambda\hat{\boldsymbol{\lambda}})\right\rangle = \begin{Bmatrix}v\mathbf{I}_c\\ \langle\mathbf{P}_n^{T}\rangle\end{Bmatrix}\hat{\boldsymbol{\varepsilon}} \qquad \text{and} \qquad \left\langle\mathbf{B}_\lambda^{T}\right\rangle\mathbf{C}\hat{\boldsymbol{\varepsilon}} = \mathbf{0}$$

(28a,b)

The constraints are :

$$\mathbf{H}_{cc} = v\mathbf{S} \quad , \quad \mathbf{H}_{cn} = \mathbf{S}\langle\mathbf{P}_n\rangle \qquad \text{and} \qquad \langle\mathbf{B}_\lambda\rangle = \mathbf{0}$$

(28c)

Furthermore, it can be checked that the consistency of Eqn.(27c) imposes no further constraint.

Consideration for (C2) : For the validity of (C2) and by making use of Eqn.(27) and Eqn.(28),

$$\oint\boldsymbol{\Gamma}^{T}\mathbf{n}\,ds\;\mathbf{C}\hat{\boldsymbol{\varepsilon}} = \left(\mathbf{G}_q^{T}\mathbf{H}^{-1}\mathbf{G}_q - \mathbf{G}_q^{T}\mathbf{H}^{-1}\mathbf{G}_\lambda(\mathbf{G}_\lambda^{T}\mathbf{H}^{-1}\mathbf{G}_\lambda)^{-1}\mathbf{G}_\lambda^{T}\mathbf{H}^{-1}\mathbf{G}_q\right)\hat{\mathbf{q}}$$

$$= \mathbf{G}_q^{T}\mathbf{H}^{-1}\left(\mathbf{G}_q\hat{\mathbf{q}}_e + \mathbf{G}_\lambda\hat{\boldsymbol{\lambda}}\right) = \mathbf{G}_q^{T}\begin{Bmatrix}\mathbf{C}\hat{\boldsymbol{\varepsilon}}\\ \mathbf{0}\end{Bmatrix} = \left\langle\mathbf{B}_q^{T}\right\rangle\mathbf{C}\hat{\boldsymbol{\varepsilon}} \qquad (29)$$

which ends up to be the same constraint as Eqn.(22b).

Consideration for (C3) : (C3) depends purely on the choice of $\boldsymbol{\Gamma}$ and does not concern $\mathbf{H}_{cc}$, $\mathbf{H}_{cn}$ and $\mathbf{H}_{nn}$.

Consideration for (C4) : For a positive definite $\mathbf{H}$ and $\boldsymbol{\varepsilon}^{u}$ possessing a proper kernal, it can be seen from Eqn.(27d) that a non-rigid body mode $\begin{bmatrix}\mathbf{q}_{NR}^{T} & \boldsymbol{\lambda}_{NR}^{T}\end{bmatrix}^{T}$ is a mechanism if and only if

$$\mathbf{G}_q\,\mathbf{q}_{NR} + \mathbf{G}_\lambda\,\boldsymbol{\lambda}_{NR} = \left\langle\begin{bmatrix}\mathbf{I}_c & \mathbf{P}_n\end{bmatrix}^{T}(\mathbf{B}_q\,\mathbf{q}_{NR} + \mathbf{B}_\lambda\,\boldsymbol{\lambda}_{NR})\right\rangle = \mathbf{0} \qquad (30a)$$

which depends purely on the choice of the stress modes (note : $\mathbf{B}_q\,\mathbf{q}_{NR}+\mathbf{B}_\lambda\,\boldsymbol{\lambda}_{NR}\neq\mathbf{0}$). Provided that

$$\left\langle\left[\mathbf{I}_c \quad \mathbf{P}_n\right]^T(\mathbf{B}_q\,\mathbf{q}+\mathbf{B}_\lambda\,\boldsymbol{\lambda})\right\rangle\neq\mathbf{0} \qquad \text{for all} \qquad \mathbf{B}_q\,\mathbf{q}+\mathbf{B}_\lambda\,\boldsymbol{\lambda}\neq\mathbf{0} \tag{30b}$$

and $\boldsymbol{\varepsilon}^u$ possesses a proper kernel, the constraints due to (C4) is that $\mathbf{H}_{nn}$ does not render $\mathbf{H}$ non-positive definite. This leaves a leeway to reduce the computational cost associated with $\mathbf{H}$.

6. Patch Test Examination of the Orthogonal Approach

In this section, the Hu-Washizu counterpart of Eqn.(24) will be considered. Moreover, (Q1) and (Q2) raised in Section 2 will be answered. The functional to be considered is :

$$\Pi^e_{\sigma\varepsilon}=\frac{1}{2}\left\langle\boldsymbol{\varepsilon}^T\mathbf{C}\boldsymbol{\varepsilon}\right\rangle-\left\langle\boldsymbol{\sigma}^T\boldsymbol{\varepsilon}\right\rangle+\left\langle\boldsymbol{\sigma}^T\boldsymbol{\varepsilon}^u\right\rangle-\int_{St}\mathbf{v}^T\mathbf{t}\,ds \tag{31a}$$

which includes With the expressions for $\boldsymbol{\varepsilon}$, $\boldsymbol{\sigma}$, $\boldsymbol{\varepsilon}^u$ and $\mathbf{v}$ in Eqn.(2), Eqn.(16) and Eqn.(14) substituted, the functional will be :

$$\Pi^e_{\sigma\varepsilon}=\frac{1}{2}\begin{Bmatrix}\boldsymbol{\alpha}_c\\ \boldsymbol{\alpha}_n\end{Bmatrix}^T\begin{bmatrix}v\mathbf{C} & \mathbf{C}\left\langle\mathbf{Q}_n\right\rangle\\ sym. & \left\langle\mathbf{Q}_n^T\mathbf{C}\mathbf{Q}_n\right\rangle\end{bmatrix}\begin{Bmatrix}\boldsymbol{\alpha}_c\\ \boldsymbol{\alpha}_n\end{Bmatrix}-\begin{Bmatrix}\boldsymbol{\beta}_c\\ \boldsymbol{\beta}_n\end{Bmatrix}^T\mathbf{W}\begin{Bmatrix}\boldsymbol{\alpha}_c\\ \boldsymbol{\alpha}_n\end{Bmatrix}+\begin{Bmatrix}\boldsymbol{\beta}_c\\ \boldsymbol{\beta}_n\end{Bmatrix}^T\left[\mathbf{G}_q \;\vdots\; \mathbf{G}_\lambda\right]\begin{Bmatrix}\mathbf{q}\\ \boldsymbol{\lambda}\end{Bmatrix}-\mathbf{q}^T\int_{St}\boldsymbol{\Gamma}^T\mathbf{t}\,ds \tag{31b}$$

The only undefined term is :

$$\mathbf{W}=\begin{bmatrix}v\mathbf{I}_c & \left\langle\mathbf{Q}_n\right\rangle\\ \left\langle\mathbf{P}_n^T\right\rangle & \left\langle\mathbf{P}_n^T\mathbf{Q}_n\right\rangle\end{bmatrix}$$

which will be assumed to be invertible. After the following replacements :

$$\begin{bmatrix}v\mathbf{C} & \mathbf{C}\left\langle\mathbf{Q}_n\right\rangle\\ sym. & \left\langle\mathbf{Q}_n^T\mathbf{C}\mathbf{Q}_n\right\rangle\end{bmatrix}\rightarrow\mathbf{M}=\begin{bmatrix}\mathbf{M}_{cc} & \mathbf{M}_{cn}\\ sym. & \mathbf{M}_{nn}\end{bmatrix} \tag{32}$$

Eqn.(31b) becomes :

$$\Pi^e_{\sigma\varepsilon}=\frac{1}{2}\begin{Bmatrix}\boldsymbol{\alpha}_c\\ \boldsymbol{\alpha}_n\end{Bmatrix}^T\mathbf{M}\begin{Bmatrix}\boldsymbol{\alpha}_c\\ \boldsymbol{\alpha}_n\end{Bmatrix}-\begin{Bmatrix}\boldsymbol{\beta}_c\\ \boldsymbol{\beta}_n\end{Bmatrix}^T\mathbf{W}\begin{Bmatrix}\boldsymbol{\alpha}_c\\ \boldsymbol{\alpha}_n\end{Bmatrix}+\begin{Bmatrix}\boldsymbol{\beta}_c\\ \boldsymbol{\beta}_n\end{Bmatrix}^T\left[\mathbf{G}_q \quad \mathbf{G}_\lambda\right]\begin{Bmatrix}\mathbf{q}\\ \boldsymbol{\lambda}\end{Bmatrix}-\mathbf{q}^T\int_{St}\boldsymbol{\Gamma}^T\mathbf{t}\,ds \tag{33}$$

Following the standard variational procedure,

$$\mathbf{W}\begin{Bmatrix}\boldsymbol{\alpha}_c\\ \boldsymbol{\alpha}_n\end{Bmatrix}=\begin{bmatrix}\mathbf{G}_q & \mathbf{G}_\lambda\end{bmatrix}\begin{Bmatrix}\mathbf{q}_e\\ \boldsymbol{\lambda}\end{Bmatrix} \quad , \quad \mathbf{W}^T\begin{Bmatrix}\boldsymbol{\beta}_c\\ \boldsymbol{\beta}_n\end{Bmatrix}=\mathbf{M}\begin{Bmatrix}\boldsymbol{\alpha}_c\\ \boldsymbol{\alpha}_n\end{Bmatrix}$$

(34a,b)

$$\mathbf{G}_\lambda^T\boldsymbol{\beta}=\left\langle\mathbf{B}_\lambda\right\rangle^T\boldsymbol{\beta}_c+\left\langle\mathbf{P}_n^T\mathbf{B}_\lambda\right\rangle^T\boldsymbol{\beta}_n=\mathbf{0} \quad , \quad \mathbf{G}_\lambda^T\mathbf{W}^{-T}\mathbf{M}\mathbf{W}^{-1}(\mathbf{G}_q\,\mathbf{q}+\mathbf{G}_\lambda\,\boldsymbol{\lambda})=\mathbf{0}$$

(34c,d)

$$\Pi_{\sigma\varepsilon}^e=\frac{1}{2}\begin{Bmatrix}\mathbf{q}\\ \boldsymbol{\lambda}\end{Bmatrix}^T\begin{bmatrix}\mathbf{G}_q & \mathbf{G}_\lambda\end{bmatrix}^T\mathbf{W}^{-T}\mathbf{M}\mathbf{W}^{-1}\begin{bmatrix}\mathbf{G}_q & \mathbf{G}_\lambda\end{bmatrix}\begin{Bmatrix}\mathbf{q}\\ \boldsymbol{\lambda}\end{Bmatrix}$$

$$=\frac{1}{2}\mathbf{q}^T\mathbf{G}_q^T\mathbf{W}^{-T}\left(\mathbf{M}-\mathbf{M}\mathbf{W}^{-1}\mathbf{G}_\lambda(\mathbf{G}_\lambda^T\mathbf{W}^{-T}\mathbf{M}\mathbf{W}^{-1}\mathbf{G}_\lambda)^{-1}\mathbf{G}_\lambda^T\mathbf{W}^{-T}\mathbf{M}\right)\mathbf{W}^{-1}\mathbf{G}_q\,\mathbf{q}-\mathbf{q}^T\int_{St}\boldsymbol{\Gamma}^T\,\mathbf{t}\,ds$$

(34e)

Consideration for (C1) : Same as last section, the existence of $\hat{\mathbf{q}}$ and $\hat{\boldsymbol{\lambda}}$ is assumed such that Eqn.(20) is valid. (C1) requires that $\boldsymbol{\alpha}_c = \hat{\boldsymbol{\varepsilon}}$, $\boldsymbol{\beta}_c = \mathbf{C}\hat{\boldsymbol{\varepsilon}}$ and $\boldsymbol{\alpha}_n = \boldsymbol{\beta}_n = \mathbf{0}$ for $\boldsymbol{\varepsilon}^u = \mathbf{B}_q\,\hat{\mathbf{q}}+\mathbf{B}_\lambda\,\hat{\boldsymbol{\lambda}}=\hat{\boldsymbol{\varepsilon}}$. From Eqn.(34a), Eqn.(34b) and Eqn.(34c),

$$\begin{bmatrix}v\mathbf{I}_c & \left\langle\mathbf{Q}_n\right\rangle\\ \left\langle\mathbf{P}_n^T\right\rangle & \left\langle\mathbf{P}_n^T\mathbf{Q}_n\right\rangle\end{bmatrix}\begin{Bmatrix}\hat{\boldsymbol{\varepsilon}}\\ \mathbf{0}\end{Bmatrix}=\begin{bmatrix}\mathbf{G}_q & \mathbf{G}_\lambda\end{bmatrix}\begin{Bmatrix}\hat{\mathbf{q}}\\ \hat{\boldsymbol{\lambda}}\end{Bmatrix}=\left\langle\begin{bmatrix}\mathbf{I}_c & \mathbf{P}_n\end{bmatrix}^T\left(\mathbf{B}_q\hat{\mathbf{q}}+\mathbf{B}_\lambda\,\hat{\boldsymbol{\lambda}}\right)\right\rangle=\begin{bmatrix}v\mathbf{I}_c\\ \left\langle\mathbf{P}_n^T\right\rangle\end{bmatrix}\hat{\boldsymbol{\varepsilon}} \qquad (35a)$$

$$\begin{bmatrix}v\mathbf{I}_c & \left\langle\mathbf{Q}_n\right\rangle\\ \left\langle\mathbf{P}_n^T\right\rangle & \left\langle\mathbf{P}_n^T\mathbf{Q}_n\right\rangle\end{bmatrix}^T\begin{Bmatrix}\mathbf{C}\hat{\boldsymbol{\varepsilon}}\\ \mathbf{0}\end{Bmatrix}=\begin{bmatrix}\mathbf{M}_{cc} & \mathbf{M}_{cn}\\ sym. & \mathbf{M}_{nn}\end{bmatrix}\begin{Bmatrix}\hat{\boldsymbol{\varepsilon}}\\ \mathbf{0}\end{Bmatrix} \quad , \quad \begin{bmatrix}\mathbf{G}_{c\lambda} & \left\langle\mathbf{P}_n^T\mathbf{B}_\lambda\right\rangle\end{bmatrix}\begin{Bmatrix}\mathbf{C}\hat{\boldsymbol{\varepsilon}}\\ \mathbf{0}\end{Bmatrix}=\mathbf{0} \qquad (35b,c)$$

Eqn.(35a) imposes no constraint but Eqn.(35b,c) imposes :

$$\mathbf{M}_{cc}=v\mathbf{C} \quad , \quad \mathbf{M}_{cn}=\mathbf{C}\left\langle\mathbf{Q}_n\right\rangle \quad , \quad \left\langle\mathbf{B}_\lambda\right\rangle=\mathbf{0}$$

(36)

Apparently, the consistency of Eqn.(34d) induces no further constraint.

Consideration for (C2) : For the veracity of (C2) and by making use of Eqn.(34), Eqn.(35) and Eqn.(35),

$$\oint\boldsymbol{\Gamma}_q^T\mathbf{n}\,ds\;\mathbf{C}\hat{\boldsymbol{\varepsilon}}=\mathbf{G}_q^T\mathbf{W}^{-T}\left(\mathbf{M}-\mathbf{M}\mathbf{W}^{-1}\mathbf{G}_\lambda(\mathbf{G}_\lambda^T\mathbf{W}^{-T}\mathbf{M}\mathbf{W}^{-1}\mathbf{G}_\lambda)^{-1}\mathbf{G}_\lambda^T\mathbf{W}^{-T}\mathbf{M}\right)\mathbf{W}^{-1}\mathbf{G}_q\hat{\mathbf{q}}$$

$$=\mathbf{G}_q^T\mathbf{W}^{-T}\mathbf{M}\mathbf{W}^{-1}\left(\mathbf{G}_q\hat{\mathbf{q}}+\mathbf{G}_\lambda\,\hat{\boldsymbol{\lambda}}\right)=\mathbf{G}_q^T\begin{Bmatrix}\mathbf{C}\hat{\boldsymbol{\varepsilon}}\\ \mathbf{0}\end{Bmatrix}=\left\langle\mathbf{B}_q^T\right\rangle\mathbf{C}\hat{\boldsymbol{\varepsilon}}$$

(37)

The constraint is the same as Eqn.(22b) and Eqn.(29).

Consideration for (C3) : (C3) depends purely on the choice of $\boldsymbol{\Gamma}$ and does not concern $\mathbf{M}_{cc}$, $\mathbf{M}_{cn}$ and $\mathbf{M}_{nn}$.

Consideration for (C4) : For a positive definite $\mathbf{M}$ and $\boldsymbol{\varepsilon}^u$ possessing a proper kernal, it can be deduced from Eqn.(34e) that a non-rigid body mode $\left[\mathbf{q}_{NR}^T \quad \boldsymbol{\lambda}_{NR}^T\right]^T$ is a mechanism if and only if

$$\mathbf{G}_q\,\mathbf{q}_{NR} + \mathbf{G}_\lambda\,\boldsymbol{\lambda}_{NR} = \left\langle \left[\mathbf{I}_c \quad \mathbf{P}_n\right]^T (\mathbf{B}_q\,\mathbf{q}_{NR} + \mathbf{B}_\lambda\,\boldsymbol{\lambda}_{NR}) \right\rangle = \mathbf{0} \tag{38a}$$

which depends purely on the choice of the stress modes (note : $\mathbf{B}_q\,\mathbf{q}_{NR} + \mathbf{B}_\lambda\,\boldsymbol{\lambda}_{NR} \neq \mathbf{0}$). Provided that

$$\left\langle \left[\mathbf{I}_c \quad \mathbf{P}_n\right]^T (\mathbf{B}_q\,\mathbf{q} + \mathbf{B}_\lambda\,\boldsymbol{\lambda}) \right\rangle \neq \mathbf{0} \qquad \text{for all} \qquad \mathbf{B}_q\,\mathbf{q} + \mathbf{B}_\lambda\,\boldsymbol{\lambda} \neq \mathbf{0} \tag{38b}$$

and $\boldsymbol{\varepsilon}^u$ possesses a proper kernel, the constraints due to (C4) is that $\mathbf{M}_{nn}$ does not render $\mathbf{M}$ non-positive definite. This deduction offers the solutions to (Q1) and (Q2) raised in Section 2 and leaves a leeway to reduce the computational cost associated with $\mathbf{M}$.

7. AMF for Lower Order Elements with Internal Displacement D.O.F.s

AMF was first applied to lower order elements with internal d.o.f.s, i.e. $\boldsymbol{\lambda}$ [14,16]. For these elements, considerable improvement in efficiency are yielded by using a similar simplification as in the orthogonal approach. The answer to (Q3) raised in Section 2 is affirmative. In Eqn.(2a), the stress modes are only decomposed into constant modes, $\mathbf{I}_c\,\boldsymbol{\beta}_c$, and non-constant modes, $\mathbf{P}_n\,\boldsymbol{\beta}_n$. In the subsequent discussion, the non-constant modes are further decomposed into the higher order modes, $\mathbf{P}_H\,\boldsymbol{\beta}_H$, and non-constant lower order modes $\mathbf{P}_l\,\boldsymbol{\beta}_l$. Moreover, the lower order modes, $\mathbf{P}_L\,\boldsymbol{\beta}_L$, is defined as the union of the constant modes and non-constant lower order modes. Symbolically,

$$\mathbf{P}_n\,\boldsymbol{\beta}_n = [\,\mathbf{P}_l \quad \mathbf{P}_H\,]\begin{Bmatrix}\boldsymbol{\beta}_l \\ \boldsymbol{\beta}_H\end{Bmatrix}, \quad \mathbf{P}_L\,\boldsymbol{\beta}_L = [\,\mathbf{I}_c \quad \mathbf{P}_l\,]\begin{Bmatrix}\boldsymbol{\beta}_c \\ \boldsymbol{\beta}_l\end{Bmatrix} \tag{39}$$

After taking Eqn.(28c) into account, Eqn.(26) can be expanded as :

$$\Pi_{\sigma}^{e}=-\frac{1}{2}\begin{Bmatrix}\boldsymbol{\beta}_c\\ \boldsymbol{\beta}_l\\ \boldsymbol{\beta}_H\end{Bmatrix}^T\begin{bmatrix} v\mathbf{S} & \mathbf{S}\langle\mathbf{P}_l\rangle & \mathbf{S}\langle\mathbf{P}_H\rangle\\ & \mathbf{H}_{ll} & \mathbf{H}_{lH}\\ sym. & & \mathbf{H}_{HH}\end{bmatrix}\begin{Bmatrix}\boldsymbol{\beta}_c\\ \boldsymbol{\beta}_l\\ \boldsymbol{\beta}_H\end{Bmatrix}+\begin{Bmatrix}\boldsymbol{\beta}_c\\ \boldsymbol{\beta}_l\\ \boldsymbol{\beta}_H\end{Bmatrix}^T\begin{bmatrix}\langle\mathbf{B}_q\rangle & \langle\mathbf{B}_\lambda\rangle\\ \langle\mathbf{P}_l^T\mathbf{B}_q\rangle & \langle\mathbf{P}_l^T\mathbf{B}_\lambda\rangle\\ \langle\mathbf{P}_H^T\mathbf{B}_q\rangle & \langle\mathbf{P}_H^T\mathbf{B}_\lambda\rangle\end{bmatrix}\begin{Bmatrix}\mathbf{q}\\ \boldsymbol{\lambda}\end{Bmatrix}-\mathbf{q}^T\int_{St}\boldsymbol{\Gamma}^T\,\mathbf{t}\,ds \tag{40a}$$

It will be assumed for lower order elements that they contain only lower order non-constant stress modes. The functional of the elements is :

$$\Pi_{\sigma}^{e}=-\frac{1}{2}\begin{Bmatrix}\boldsymbol{\beta}_c\\ \boldsymbol{\beta}_l\end{Bmatrix}^T\begin{bmatrix} v\mathbf{S} & \mathbf{S}\langle\mathbf{P}_l\rangle\\ sym. & \mathbf{H}_{ll}\end{bmatrix}\begin{Bmatrix}\boldsymbol{\beta}_c\\ \boldsymbol{\beta}_l\end{Bmatrix}+\begin{Bmatrix}\boldsymbol{\beta}_c\\ \boldsymbol{\beta}_l\end{Bmatrix}^T\begin{bmatrix}\langle\mathbf{B}_q\rangle & \langle\mathbf{B}_\lambda\rangle\\ \langle\mathbf{P}_l^T\mathbf{B}_q\rangle & \langle\mathbf{P}_l^T\mathbf{B}_\lambda\rangle\end{bmatrix}\begin{Bmatrix}\mathbf{q}\\ \boldsymbol{\lambda}\end{Bmatrix}\qquad -\mathbf{q}^T\int_{St}\boldsymbol{\Gamma}^T\,\mathbf{t}\,ds \tag{40b}$$

In particular, if

$$\mathbf{P}_l=\begin{bmatrix}\mathbf{I}_c f_1 & \mathbf{I}_c f_2 & \cdots & \mathbf{I}_c f_m\end{bmatrix} \tag{41a}$$

in which

$$\langle f_i\rangle=0 \qquad \text{for any } J \quad , \quad \langle f_i f_j\rangle=0 \quad \text{for} \quad i\neq j \quad \text{and} \quad J \quad \text{being a constant} \tag{41b}$$

and $\mathbf{H}_{ll}$ is taken to be :

$$\mathbf{H}_{ll}=diag.\begin{Bmatrix}\langle f_1^2\rangle\mathbf{S} & \cdots & \langle f_m^2\rangle\mathbf{S}\end{Bmatrix} \tag{41c}$$

we have

$$\Pi_{\sigma}^{e}=\frac{1}{2}\begin{Bmatrix}\mathbf{q}\\ 1\end{Bmatrix}^T\left(\frac{1}{v}\begin{bmatrix}\langle\mathbf{B}_q^T\langle\mathbf{C}\rangle\mathbf{B}_q\langle & \mathbf{0}\\ \mathbf{0} & \mathbf{0}\end{bmatrix}+\sum_{i=1}^{m}\langle f_i^2\langle\begin{bmatrix}\langle\mathbf{P}_l^T\mathbf{B}_q\langle & \langle\mathbf{P}_l^T\mathbf{B}_\lambda\langle\end{bmatrix}^T\mathbf{C}\begin{bmatrix}\langle\mathbf{P}_l^T\mathbf{B}_q\langle & \langle\mathbf{P}_l^T\mathbf{B}_\lambda\langle\end{bmatrix}\right)\begin{Bmatrix}\mathbf{q}\\ 1\end{Bmatrix}-\mathbf{q}^T\int_{St}\mathrm{G}^T\,\mathbf{t}ds \tag{42}$$

Comparing the generalized element stiffness matrix (inside the parenthesis) with that in Eqn.(12), the present *AMF* should be more efficient than the orthogonal approach.

8. AMF for Lower Order Elements with no Internal D.O.F.s

A drawback of the orthogonal approach and *AMF* for lower order elements with $\boldsymbol{\lambda}$ is the condensation cost incurred by $\boldsymbol{\lambda}$. When $\boldsymbol{\lambda}$ does not exist, Eqn.(40b) reduces to :

$$\Pi_{\sigma}^{e} = \frac{1}{2}\mathbf{q}^{T}\left(\frac{1}{v}\left\langle \mathbf{B}_{q}^{T}\right\rangle \mathbf{C}\left\langle \mathbf{B}_{q}\right\rangle + \left\langle \mathbf{P}_{l}^{T}\mathbf{B}_{q}\right\rangle^{T}\mathbf{H}_{ll}^{-1}\left\langle \mathbf{P}_{l}^{T}\mathbf{B}_{q}\right\rangle\right)\mathbf{q} - \mathbf{q}^{T}\int_{St}\boldsymbol{\Gamma}^{T}\,\mathbf{t}\,ds \qquad (43)$$

A necessity condition for the stability of a hybrid stress element is :

$$dim.(\boldsymbol{\beta}) \;\geq\; dim.(\mathbf{q}) + dim.(\boldsymbol{\lambda}) - number\ of\ rigid\ body\ modes \qquad (44)$$

which is the well-known *LBB condition* [40,41]. Taking the 8-node brick as an example, a stable element in the absence of internal d.o.f.s requires a minimum of 18 stress modes to secure its stability. When 9 internal d.o.f.s are introduced [14,16,17], the minimal dim.($\boldsymbol{\beta}$) increases to 27. A total of 36 (9 in $\boldsymbol{\lambda}$ and 27 in $\boldsymbol{\beta}$) internal coefficients have to be condensed instead of 18 in the element with no internal d.o.f.s.

The application of *AMF* to Pian & Tong's 8-node brick [20,42,43] is demonstrated. In this and the subsequently introduced elements, $\mathbf{B}_q = \mathbf{D}\mathbf{N}_q$ and $\boldsymbol{\Gamma} = \mathbf{N}_q$ where $\mathbf{N}_q$ is the standard displacement interpolation matrix. The non-constant stress modes of Pian & Tong's 8-node brick in the natural coordinates (ξ,η,ζ) contain the following uncoupled modes :

$$\sigma_{\xi\xi} = \eta,\zeta,\eta\zeta \;;\; \sigma_{\eta\eta} = \zeta,\xi,\zeta\xi \;;\; \sigma_{\zeta\zeta} = \xi,\eta,\xi\eta \;;\; \sigma_{\eta\zeta} = \xi \;;\; \sigma_{\zeta\xi} = \eta \;;\; \sigma_{\xi\eta} = \zeta \qquad (45a)$$

The non-constant Cartesian stress $\boldsymbol{\sigma}_l = [\sigma_{xx}\ \sigma_{yy}\ \sigma_{zz}\ \sigma_{yz}\ \sigma_{zx}\ \sigma_{xy}]_l^T = \mathbf{P}_l\,\boldsymbol{\beta}_l$ is obtained from $[\sigma_{\xi\xi}\ \sigma_{\eta\eta}\ \sigma_{\zeta\zeta}\ \sigma_{\eta\zeta}\ \sigma_{\zeta\xi}\ \sigma_{\xi\eta}]^T$ via the contravariant stress transformation matrix $\mathbf{T}_{\sigma}$ evaluated at the element origin, i.e.

$$\mathbf{P}_l = \left[f_1\mathbf{P}_1 \quad f_2\mathbf{P}_2 \quad f_3\mathbf{P}_3 \quad f_4\mathbf{T}_1 \quad f_5\mathbf{T}_2 \quad f_6\mathbf{T}_3\right] \quad , \quad \boldsymbol{\beta}_l = \left[\boldsymbol{\beta}_1^T \quad \boldsymbol{\beta}_2^T \quad \boldsymbol{\beta}_3^T \quad \beta_4 \quad \beta_5 \quad \beta_6\right]^T \qquad (45b)$$

where

$$\mathbf{P}_1 = [\,\mathbf{T}_2 \quad \mathbf{T}_3 \quad \mathbf{T}_4\,], \quad \mathbf{P}_2 = [\,\mathbf{T}_3 \quad \mathbf{T}_1 \quad \mathbf{T}_5\,], \quad \mathbf{P}_3 = [\,\mathbf{T}_1 \quad \mathbf{T}_2 \quad \mathbf{T}_6\,]$$
$$[\,\mathbf{T}_1 \quad \mathbf{T}_2 \quad \mathbf{T}_3 \quad \mathbf{T}_4 \quad \mathbf{T}_5 \quad \mathbf{T}_6\,] = \mathbf{T}_{\sigma}(\xi=\eta=\zeta=0)$$

The original and the two possible sets of f_i's [42-45] that satisfied the criteria laid down in Eqn.(41b) are :

original : $f_1 = \xi$, $f_2 = \eta$, $f_3 = \zeta$, $f_4 = \eta\zeta$, $f_5 = \zeta\xi$, $f_6 = \xi\eta$

1st orthogonal choice : $f_1 = \xi / J$, $f_2 = \eta / J$, $f_3 = \zeta / J$, $f_4 = \eta\zeta / J$, $f_5 = \zeta\xi / J$, $f_6 = \xi\eta / J$

2nd orthogonal choice : $f_1 = \xi - \langle\xi\rangle / v$, $f_2 = \eta - \langle\eta\rangle / v$, $f_3 = \zeta - \langle\zeta\rangle / v$

$$f_4 = \eta\zeta - \langle \eta\zeta \rangle / v \ , \ f_5 = \zeta\xi - \langle \zeta\xi \rangle / v \ , \ f_6 = \xi\eta - \langle \xi\eta \rangle / v$$

By retaining only the terms which do not vanish for constant J's in $\langle \mathbf{P}_l^T \mathbf{S} \mathbf{P}_l \rangle$, it becomes

$$\mathbf{H}_{ll} = diag.\{\mathbf{H}_1, \mathbf{H}_2, \mathbf{H}_3, H_4, H_5, H_6\} \tag{46}$$

where

$$\mathbf{H}_1 = \langle f_1^2 \rangle \begin{bmatrix} S_{22}^* & S_{23}^* & S_{24}^* \\ & S_{33}^* & S_{34}^* \\ sym. & & S_{44}^* \end{bmatrix} , \ \mathbf{H}_2 = \langle f_2^2 \rangle \begin{bmatrix} S_{33}^* & S_{31}^* & S_{35}^* \\ & S_{11}^* & S_{15}^* \\ sym. & & S_{55}^* \end{bmatrix} , \ \mathbf{H}_3 = \langle f_3^2 \rangle \begin{bmatrix} S_{11}^* & S_{12}^* & S_{16}^* \\ & S_{22}^* & S_{26}^* \\ sym. & & S_{66}^* \end{bmatrix}$$

$$H_4 = \langle f_4^2 \rangle S_{11}^* \ , \ H_5 = \langle f_5^2 \rangle S_{22}^* \ , \ H_6 = \langle f_6^2 \rangle S_{33}^* \ ,$$

$$\mathbf{S}^* = [S_{ij}^*] = \mathbf{T}_\sigma^T(\xi = \eta = \zeta = 0)\, \mathbf{S}\, \mathbf{T}_\sigma(\xi = \eta = \zeta = 0)$$

With the above $\mathbf{H}_{ll}$, Eqn.(43) can be expanded as :

$$\Pi_\sigma^e = \frac{1}{2}\mathbf{q}^T \left(\frac{1}{v} \langle \mathbf{B}_q^T \rangle \mathbf{C} \langle \mathbf{B}_q \rangle + \sum_{i=1}^{3} \langle f_i \mathbf{B}_q^T \rangle \mathbf{P}_i^T \mathbf{H}_i^{-1} \mathbf{P}_i \langle f_i \mathbf{B}_q \rangle + \sum_{i=1}^{3} \frac{1}{H_i} \langle f_{i+3} \mathbf{B}_q^T \rangle \mathbf{T}_i^T \mathbf{T}_i \langle f_{i+3} \mathbf{B}_q \rangle \right) \mathbf{q} - \mathbf{q}^T \int_{St} \mathbf{\Gamma}^T \mathbf{t}\, ds \tag{47}$$

Thus, only three 3x3 symmetric matrices have to be inverted instead of a 18x18 symmetric matrix in the parent model of Pian & Tong. Moreover, the sparsity in $\mathbf{H}_{ll}$ also significantly reduces the number of arithmetic operations. To construct the present element, only 82% of the CPU time required to construct Q8, the standard 8-node displacement-based element, is consumed [43]. As revealed by a number of numerical examples, the accuracy of the element is only marginally lower than that of its parent element [42,43].

A selective scaling technique has also been developed within the context of *AMF* to circumvent the locking problems encountered by this brick element in thin plate/shell analysis [42,44,45]. The scaled element in some problems is even more accurate than Bathe & Dvorkin's MITC4 4-node assumed natural strain shell element [30]. Table 1 lists the central deflections of a clamped circular plate subjected to a central point load, see Fig.2 for the employed meshes. The tabulated deflections have been normalized by the analytical result given by Timoshenko [46]. The *AMF* shell element is a 4-node (5 d.o.f. per node) hybrid stress element making use of the transverse shear strain field of MITC4 and it is less stiff than MITC4 [47]. Obviously, the present *AMF* solid element is close to the *AMF* shell element in accuracy.

mesh density	Q8	QM6-3/D [34]	Pian & Tong [20]	*AMF* solid [43]	*AMF* shell [47]

N = 3	0.006	0.116	0.517	0.846	0.890
N = 12	0.020	0.579	0.869	0.947	0.967
N = 48	0.072	0.926	0.983	0.989	0.991

Table 1 Normalized deflections for clamped circular plate subjected to central point load, see Fig.2

9. Issues to be Resolved on Extending AMF to Higher Order Elements

In Eqn.(40a), the legitimate counterpart of the submatrix formed by $\mathbf{H}_{ll}$, $\mathbf{H}_{lH}$ and $\mathbf{H}_{HH}$ is $\left\langle \mathbf{P}_n^T \mathbf{S} \mathbf{P}_n \right\rangle$. For a lower order element, it contains only a small number of non-constant stress modes and its J is a low order polynomial. Therefore, the practice of cancelling the entries in $\left\langle \mathbf{P}_n^T \mathbf{S} \mathbf{P}_n \right\rangle$ that vanish when J is constant induces only minor change in $\left\langle \mathbf{P}_n^T \mathbf{S} \mathbf{P}_n \right\rangle$ and thus the element accuracy. For higher order elements, a number of issues have to be resolved :

- a large number of stress modes have to be determined and condensed.
- the adopted practice of simplifying $\left\langle \mathbf{P}_n^T \mathbf{S} \mathbf{P}_n \right\rangle$ for lower order elements does not yield satisfactory computational saving.
- due to the higher order nature of J, the adopted practice of simplifying $\left\langle \mathbf{P}_n^T \mathbf{S} \mathbf{P}_n \right\rangle$ for lower order elements sometimes results in peculiar predictions.
- making use of the Gram-Schmidt scheme to achieve additional stress orthogonality is possible but cumbersome .

10. Rhiu & Lee's Hybrid Stabilization

The idea for a satisfactory way of extending *AMF* to higher order element came from Rhiu & Lee's approach for improving the computational efficiency of hybrid strain element [48,49]. The approach has been employed to design higher order elements for plate/shell analysis [48,50,51] and is based on the strain-version of the Hellinger-Reissner functional :

$$\Pi_{\varepsilon}^{e} = -\frac{1}{2}\left\langle \boldsymbol{\varepsilon}^T \mathbf{C} \boldsymbol{\varepsilon} \right\rangle + \left\langle \boldsymbol{\varepsilon}^T \mathbf{C} \boldsymbol{\varepsilon}_q \right\rangle - \int_{St} \mathbf{v}^T \mathbf{t}\, ds \tag{48}$$

As given previously in Eqn.(16b) and Eqn.(14), $\boldsymbol{\varepsilon}_q = \mathbf{B}_q\, \mathbf{q}$ and $\mathbf{v} = \boldsymbol{\Gamma} \mathbf{q}$. By partitioning the assumed strain into the lower and higher order modes :

$$\boldsymbol{\varepsilon} = \boldsymbol{\varepsilon}_L + \boldsymbol{\varepsilon}_H \tag{49}$$

and applying the standard order of integration, Eqn.(48) becomes :

$$\Pi_{\varepsilon}^{e} = -\frac{1}{2}\left\langle \boldsymbol{\varepsilon}_L^T \mathbf{C}\boldsymbol{\varepsilon}_L \right\rangle_L - \frac{1}{2}\left\langle \boldsymbol{\varepsilon}_H^T \mathbf{C}\boldsymbol{\varepsilon}_H \right\rangle_H - \left\langle \boldsymbol{\varepsilon}_H^T \mathbf{C}\boldsymbol{\varepsilon}_L \right\rangle_L + \left\langle \boldsymbol{\varepsilon}_L^T \mathbf{C}\mathbf{B}_q \right\rangle_L \mathbf{q}_e + \left\langle \boldsymbol{\varepsilon}_H^T \mathbf{C}\mathbf{B}_q \right\rangle_H \mathbf{q} - \mathbf{q}^T \int_{St} \boldsymbol{\Gamma}^T \mathbf{t}\, ds$$

(50)

where $\langle\ \rangle_L$ and $\langle\ \rangle_H$ indicate that the integrations are performed by using the lower (sub-) and higher (full) order quadratures, respectively. Rhiu & Lee take $\boldsymbol{\varepsilon}_L$ to be the interpolated $\boldsymbol{\varepsilon}_q$ at the sub-integration points whereas the higher order strain modes are explicitly assumed, i.e.

$$\boldsymbol{\varepsilon}_L = \sum_{i=1}^{n_L} N_i \mathbf{B}_q(i)\ \mathbf{q} \qquad , \qquad \boldsymbol{\varepsilon}_H = \mathbf{Q}_H \boldsymbol{\alpha}_H$$

(51)

in which n_L is the number of sub-integration points, N_i is the interpolation function (polynomial of the natural coordinates) for the i-th sub-integration point and $N_i\ (j) = \delta_{ij}$. The index inside the parenthesis indicates that the preceded quantity is evaluated at the corresponding sub-integration point. Substitution of Eqn.(51) into Eqn.(50) gives :

$$\Pi_{\varepsilon}^{e} = \frac{1}{2}\mathbf{q}^T \left\langle \mathbf{B}_q^T \mathbf{C}\mathbf{B}_q \right\rangle_L \mathbf{q} - \frac{1}{2}\boldsymbol{\alpha}_H^T \left\langle \mathbf{Q}_H^T \mathbf{C}\mathbf{Q}_H \right\rangle_H \boldsymbol{\alpha}_H + \boldsymbol{\alpha}_H^T \left(\left\langle \mathbf{Q}_H^T \mathbf{C}\mathbf{B}_q \right\rangle_H - \left\langle \mathbf{Q}_H^T \mathbf{C}\mathbf{B}_q \right\rangle_L \right) \mathbf{q} - \mathbf{q}^T \int_{St} \boldsymbol{\Gamma}^T \mathbf{t}\, ds \tag{52}$$

Variation of $\boldsymbol{\alpha}_H$ enforces,

$$\boldsymbol{\alpha}_H = \left\langle \mathbf{Q}_H^T \mathbf{C}\mathbf{Q}_H \right\rangle_H^{-1} \left(\left\langle \mathbf{Q}_H^T \mathbf{C}\mathbf{B}_q \right\rangle_H - \left\langle \mathbf{Q}_H^T \mathbf{C}\mathbf{B}_q \right\rangle_L \right) \mathbf{q} \tag{53}$$

and the element stiffness matrix is derived as :

$$\mathbf{K} = \left\langle \mathbf{B}_q^T \mathbf{C}\mathbf{B}_q \right\rangle_L + \left(\left\langle \mathbf{Q}_H^T \mathbf{C}\mathbf{B}_q \right\rangle_H - \left\langle \mathbf{Q}_H^T \mathbf{C}\mathbf{B}_q \right\rangle_L \right)^T \left\langle \mathbf{Q}_H^T \mathbf{C}\mathbf{Q}_H \right\rangle_H^{-1} \left(\left\langle \mathbf{Q}_H^T \mathbf{C}\mathbf{B}_q \right\rangle_H - \left\langle \mathbf{Q}_H^T \mathbf{C}\mathbf{B}_q \right\rangle_L \right) \tag{54}$$

Finally, the element stress is computed by consolidating Eqn(49), Eqn.(51) and Eqn.(53) :

$$\mathbf{C}\boldsymbol{\varepsilon} = \mathbf{C}\sum_{i=1}^{n_L} N_i \mathbf{B}_q(i)\ \mathbf{q} + \mathbf{C}\mathbf{Q}_H \left\langle \mathbf{Q}_H^T \mathbf{C}\mathbf{Q}_H \right\rangle_H^{-1} \left(\left\langle \mathbf{Q}_H^T \mathbf{C}\mathbf{B}_q \right\rangle_H - \left\langle \mathbf{Q}_H^T \mathbf{C}\mathbf{B}_q \right\rangle_L \right) \mathbf{q} \tag{55}$$

It can be seen in Eqn.(54) that the row vectors in $\left\langle \mathbf{Q}_H^T \mathbf{C}\mathbf{B}_q \right\rangle_H - \left\langle \mathbf{Q}_H^T \mathbf{C}\mathbf{B}_q \right\rangle_L$ play the role of stabilizing the sub-integrated element $\left\langle \mathbf{B}_q^T \mathbf{C}\mathbf{B}_q \right\rangle_L$. The method of using an explicitly assumed

stress/strain to derive stabilization vectors will be termed *hybrid stabilization* and is different from the well-known *γ-stabilization* in the sense that the central theme of the latter is to obtain some *γ-vectors* or *γ-stabilization vectors* by means of the Gram-Schmidt scheme. After being orthogonalized with respect to the linear or even quadratic displacement field, the cross products of the *γ-vectors* are added to the sub-integrated element [52-54].

As a simple illustration of Rhiu & Lee's *hybrid stabilization*, the 9-node plane element of dimension 2x2 is considered, see Fig.3. For the sake of stabilizing the sub-integrated (by 2nd order quadrature) element, the assumed higher order strain is determined with reference to the element's mechanisms :

$$\begin{Bmatrix} u_\xi \\ u_\eta \end{Bmatrix} = \begin{bmatrix} (3\xi^2-1)(3\eta^2-1) & 0 & \xi(3\eta^2-1) \\ 0 & (3\xi^2-1)(3\eta^2-1) & -\eta(3\xi^2-1) \end{bmatrix} \begin{Bmatrix} \phi_1 \\ \phi_2 \\ \phi_3 \end{Bmatrix} \tag{56}$$

where ϕ_i 's are linear combinations of the nodal displacements. The derived strain is :

$$\begin{Bmatrix} \partial_\xi u_\xi \\ \partial_\eta u_\eta \\ \partial_\eta u_\xi + \partial_\xi u_\eta \end{Bmatrix} = \begin{bmatrix} 6\xi(3\eta^2-1) & 0 & (3\eta^2-1) \\ 0 & 6\eta(3\xi^2-1) & -(3\xi^2-1) \\ 6\eta(3\xi^2-1) & 6\xi(3\eta^2-1) & 0 \end{bmatrix} \begin{Bmatrix} \phi_1 \\ \phi_2 \\ \phi_3 \end{Bmatrix} \tag{57}$$

The last mode is suppressed automatically when two or more elements are used in a mesh, i.e. it is non-commutable. The higher order assumed strains chosen by Lee & Rhiu [49] are :

$$\boldsymbol{\varepsilon}_H = \begin{Bmatrix} \varepsilon_{xx} \\ \varepsilon_{yy} \\ 2\varepsilon_{xy} \end{Bmatrix}_H = \mathbf{T}_\varepsilon \begin{bmatrix} \xi\eta^2 & 0 \\ 0 & \eta\xi^2 \\ 0 & 0 \end{bmatrix} \boldsymbol{\alpha}_H \tag{58}$$

where $\mathbf{T}_\varepsilon$ is their employed strain transformation matrix.

11. AMF version of Hybrid Stabilization

The relation between the assumed strain and the displacement-derived strain is conventionally obtained by variational enforcement. This is different from the direct intervention in Eqn.(51). However, Rhiu & Lee's idea is seminal in circumventing the unresolved issues outlined in Section 9.

Instead of using orthogonal constant and non-constant stress modes in *AMF*, orthogonal lower and higher order modes are employed, i.e.

$$\left\langle \mathbf{P}_L^T \mathbf{P}_H \right\rangle = \mathbf{0} \qquad \text{or equivalently,} \qquad \left\langle \mathbf{P}_l^T \mathbf{P}_H \right\rangle = \mathbf{0} \;\; \text{and} \;\; \left\langle \mathbf{P}_H \right\rangle = \mathbf{0} \qquad (59a,b)$$

Moreover, the legitimate counterpart of $\mathbf{H}_{ll}$ is employed. Since internal (displacement) d.o.f.s are rarely employed in higher order elements, they will be discarded for the subsequent discussions. Thus, Eqn.(40a) reduces to :

$$\Pi_\sigma^e = -\frac{1}{2}\begin{Bmatrix} \boldsymbol{\beta}_c \\ \boldsymbol{\beta}_l \\ \boldsymbol{\beta}_H \end{Bmatrix}^T \begin{bmatrix} v\mathbf{S} & \mathbf{S}\left\langle \mathbf{P}_l \right\rangle & \mathbf{0} \\ & \left\langle \mathbf{P}_l^T \mathbf{S} \mathbf{P}_l \right\rangle & \mathbf{0} \\ \textit{sym.} & & \mathbf{H}_{HH} \end{bmatrix} \begin{Bmatrix} \boldsymbol{\beta}_c \\ \boldsymbol{\beta}_l \\ \boldsymbol{\beta}_H \end{Bmatrix} + \begin{Bmatrix} \boldsymbol{\beta}_c \\ \boldsymbol{\beta}_l \\ \boldsymbol{\beta}_H \end{Bmatrix}^T \begin{bmatrix} \left\langle \mathbf{B}_q \right\rangle \\ \left\langle \mathbf{P}_l^T \mathbf{B}_q \right\rangle \\ \left\langle \mathbf{P}_H^T \mathbf{B}_q \right\rangle \end{bmatrix} \mathbf{q} - \mathbf{q}^T \int_{St} \boldsymbol{\Gamma}^T \mathbf{t}\, ds$$

(60a)

or

$$\Pi_\sigma^e = -\frac{1}{2}\begin{Bmatrix} \boldsymbol{\beta}_L \\ \boldsymbol{\beta}_H \end{Bmatrix}^T \begin{bmatrix} \left\langle \mathbf{P}_L^T \mathbf{S} \mathbf{P}_L \right\rangle & \mathbf{0} \\ \mathbf{0} & \mathbf{H}_{HH} \end{bmatrix} \begin{Bmatrix} \boldsymbol{\beta}_L \\ \boldsymbol{\beta}_H \end{Bmatrix} + \begin{Bmatrix} \boldsymbol{\beta}_L \\ \boldsymbol{\beta}_H \end{Bmatrix}^T \begin{bmatrix} \left\langle \mathbf{P}_L^T \mathbf{B}_q \right\rangle \\ \left\langle \mathbf{P}_H^T \mathbf{B}_q \right\rangle \end{bmatrix} \mathbf{q} \;\; -\mathbf{q}^T \int_{St} \boldsymbol{\Gamma}^T \mathbf{t}\, ds$$

(60b)

where $\mathbf{P}_L$ equals [$\mathbf{I}_c$ $\mathbf{P}_l$] as noted in Eqn.(39). The variational enforcements of $\boldsymbol{\beta}$'s are :

$$\boldsymbol{\beta}_L = \left\langle \mathbf{P}_L^T \mathbf{S} \mathbf{P}_L \right\rangle^{-1} \left\langle \mathbf{P}_L^T \mathbf{B}_q \right\rangle \mathbf{q} \quad , \quad \boldsymbol{\beta}_H = \mathbf{H}_{HH}^{-1} \left\langle \mathbf{P}_H^T \mathbf{B}_q \right\rangle \mathbf{q} \qquad (61a)$$

$$\Pi_\sigma^e = \frac{1}{2}\mathbf{q}^T (\mathbf{K}_L + \mathbf{K}_H)\mathbf{q} \;\; -\mathbf{q}^T \int_{St} \boldsymbol{\Gamma}^T \mathbf{t}\, ds \qquad (61b)$$

where

$$\mathbf{K}_L = \left\langle \mathbf{P}_L^T \mathbf{B}_q \right\rangle^T \left\langle \mathbf{P}_L^T \mathbf{S} \mathbf{P}_L \right\rangle^{-1} \left\langle \mathbf{P}_L^T \mathbf{B}_q \right\rangle \quad , \quad \mathbf{K}_H = \left\langle \mathbf{P}_H^T \mathbf{B}_q \right\rangle^T \mathbf{H}_{HH}^{-1} \left\langle \mathbf{P}_H^T \mathbf{B}_q \right\rangle$$

are the lower and higher order stiffness matrices, respectively. After solving $\mathbf{q}$, the stress can be computed as :

$$\boldsymbol{\sigma} = \mathbf{P}_L \boldsymbol{\beta}_L + \mathbf{P}_H \boldsymbol{\beta}_H = \mathbf{P}_L \left\langle \mathbf{P}_L^T \mathbf{S} \mathbf{P}_L \right\rangle^{-1} \left\langle \mathbf{P}_L^T \mathbf{B}_q \right\rangle \mathbf{q} + \mathbf{P}_H \mathbf{H}_{HH}^{-1} \left\langle \mathbf{P}_H^T \mathbf{B}_q \right\rangle \mathbf{q} \qquad (62)$$

To reduce the cost incurred by the lower order stiffness matrix, the lower order stress modes are chosen such that $\mathbf{K}_L$ is identical to the sub-integrated element [55]. First of all, we note that the sub-integrated element matrix and its element stress at the sub-integration points can be expressed as :

$$\left\langle \mathbf{B}_q^T \mathbf{C}\mathbf{B}_q \right\rangle_L = \sum_{i=1}^{n_L} w(i) J(i) \mathbf{B}_q^T(i) \mathbf{C}\mathbf{B}_q(i) = \overline{\mathbf{B}}^T \overline{\mathbf{S}}^{-1} \overline{\mathbf{B}} \quad , \quad \begin{Bmatrix} \mathbf{C}\mathbf{B}_q(1) \\ \vdots \\ \mathbf{C}\mathbf{B}_q(n_L) \end{Bmatrix} \mathbf{q}_e = \overline{\mathbf{S}}^{-1} \overline{\mathbf{B}}\, \mathbf{q} \quad (63)$$

where

$$\overline{\mathbf{B}} = \begin{bmatrix} w(1)J(1)\mathbf{B}_q(1) \\ \vdots \\ w(n_L)J(n_L)\mathbf{B}_q(n_L) \end{bmatrix} \quad , \quad \overline{\mathbf{S}} = diag.\left\{ w(1)J(1)\mathbf{S} \quad \cdots \quad w(n_L)J(n_L)\mathbf{S} \right\}$$

$w(i)$ is the weighting factor for the i-th sub-integration point

On the other hand,

$$\left\langle \mathbf{P}_L^T \mathbf{B}_q \right\rangle_L = \sum_{i=1}^{n} w(i) J(i) \mathbf{P}_L^T(i) \mathbf{B}_q(i) = \overline{\mathbf{P}}^T \overline{\mathbf{B}} \qquad , \qquad \left\langle \mathbf{P}_L^T \mathbf{S}\mathbf{P}_L \right\rangle_L = \sum_{i=1}^{n_L} w(i) J(i) \mathbf{P}_L^T(i) \mathbf{S}\mathbf{P}_L(i) = \overline{\mathbf{P}}^T \overline{\mathbf{S}\mathbf{P}}$$

(64)

where

$$\overline{\mathbf{P}}^T = \left[\mathbf{P}_L^T(1) \quad \cdots \quad \mathbf{P}_L^T(n_L) \right]$$

If $\overline{\mathbf{P}}$ is invertible,

$$\boldsymbol{\beta}_L = \left\langle \mathbf{P}_L^T \mathbf{S}\mathbf{P}_L \right\rangle^{-1} \left\langle \mathbf{P}_L^T \mathbf{B}_q \right\rangle \mathbf{q} = \left(\overline{\mathbf{P}}^T \overline{\mathbf{S}\mathbf{P}} \right)^{-1} \overline{\mathbf{P}}^T \overline{\mathbf{B}}\, \mathbf{q} = \overline{\mathbf{P}}^{-1} \overline{\mathbf{S}}^{-1} \overline{\mathbf{B}}\, \mathbf{q} \quad (65a)$$

$$\mathbf{K}_L = \left\langle \mathbf{P}_L^T \mathbf{B}_q \right\rangle^T \left\langle \mathbf{P}_L^T \mathbf{S}\mathbf{P}_L \right\rangle^{-1} \left\langle \mathbf{P}_L^T \mathbf{B}_q \right\rangle = \overline{\mathbf{B}}^T \overline{\mathbf{P}} \left(\overline{\mathbf{P}}^T \overline{\mathbf{S}\mathbf{P}} \right)^{-1} \overline{\mathbf{P}}^T \overline{\mathbf{B}} = \overline{\mathbf{B}}^T \overline{\mathbf{S}}^{-1} \overline{\mathbf{B}} = \left\langle \mathbf{B}_q^T \mathbf{C}\mathbf{B}_q \right\rangle_L \quad (65b)$$

and the element stress at the sub-integration points is :

$$\begin{Bmatrix} \boldsymbol{\sigma}(1) \\ \vdots \\ \boldsymbol{\sigma}(n_L) \end{Bmatrix} = \begin{Bmatrix} \mathbf{P}_L(1) \\ \vdots \\ \mathbf{P}_L(n_L) \end{Bmatrix} \boldsymbol{\beta}_L + \begin{Bmatrix} \mathbf{P}_H(1) \\ \vdots \\ \mathbf{P}_H(n_L) \end{Bmatrix} \boldsymbol{\beta}_H = \begin{Bmatrix} \mathbf{C}\mathbf{B}_q(1) \\ \vdots \\ \mathbf{C}\mathbf{B}_q(n_L) \end{Bmatrix} \mathbf{q} + \begin{Bmatrix} \mathbf{P}_H(1) \\ \vdots \\ \mathbf{P}_H(n_L) \end{Bmatrix} \mathbf{H}_{HH}^{-1} \left\langle \mathbf{P}_H^T \mathbf{B}_q \right\rangle \mathbf{q} \quad (65c)$$

The most straightforward choice of $\mathbf{P}_L$ is to employ the same set of n_L least order uncoupled polynomial terms for every stress components. Similar derivation was first given by Malkus & Hughes [56].

The last issue to be resolved is how to select the higher order stress modes which are orthogonal to the lower order ones without resorting to the Gram-Schmidt scheme. It will be seen from the following two illustrations that the proposed procedure is indeed straight forward.

11.1 Nine-Node Plane Element It can be checked that the following assumed lower order stress shape function results in an invertible $\overline{\mathbf{P}}$:

$$\mathbf{P}_L = [\ \mathbf{I}_3 \quad \xi\mathbf{I}_3 \quad \eta\mathbf{I}_3 \quad \xi\eta\mathbf{I}_3\ ] \tag{66}$$

For the 9-node plane element, the strain derived from the mechanisms of the sub-integrated element has been given in Eqn.(57). The two commutable mechanisms can be stabilized by either :

$$\begin{Bmatrix} \sigma_{\xi\xi} \\ \sigma_{\eta\eta} \\ \sigma_{\xi\eta} \end{Bmatrix}_H = \begin{bmatrix} \xi(3\eta^2-1) & 0 \\ 0 & \eta(3\xi^2-1) \\ \eta(3\xi^2-1) & \xi(3\eta^2-1) \end{bmatrix} \boldsymbol{\beta}_H \qquad \text{or} \qquad \begin{Bmatrix} \sigma_{\xi\xi} \\ \sigma_{\eta\eta} \\ \sigma_{\xi\eta} \end{Bmatrix}_H = \begin{bmatrix} \xi(3\eta^2-1) & 0 \\ 0 & \eta(3\xi^2-1) \\ 0 & 0 \end{bmatrix} \boldsymbol{\beta}_H \tag{67a}$$

In reference [55], the last assumed contravariant stress field is adopted as it is simpler and does not involve any shear terms which are detrimental to the element's bending response. The Cartesian stress is obtained as :

$$\begin{Bmatrix} \sigma_{xx} \\ \sigma_{yy} \\ \sigma_{xy} \end{Bmatrix}_H = \frac{1}{J}\mathbf{T}_\sigma(\xi=\eta=0)\begin{Bmatrix} \sigma_{\xi\xi} \\ \sigma_{\eta\eta} \\ \sigma_{\xi\eta} \end{Bmatrix}_H = \frac{1}{J}\mathbf{T}_\sigma(\xi=\eta=0)\begin{bmatrix} \xi(3\eta^2-1) & 0 \\ 0 & \eta(3\xi^2-1) \\ 0 & 0 \end{bmatrix} \boldsymbol{\beta}_H = \mathbf{P}_H\boldsymbol{\beta}_H \tag{67b}$$

Again, $\mathbf{T}_\sigma$ denotes the contravariant stress transformation matrix. The reciprocal of J is included to ensure the orthogonality between $\mathbf{P}_H$ and the $\mathbf{P}_L$ given in Eqn.(66). Using the above procedure, $\mathbf{P}_H$ also vanishes at the sub-integration points. This simplifies Eqn.(65c) to :

$$\boldsymbol{\sigma}(i) = \mathbf{C}\mathbf{B}_q(i)\,\mathbf{q} \tag{68}$$

As sub-integration points are often the super-convergent stress points, it is very common to simply interpolate/extrapolate the stress values at these points in computing the element stress. Under this practice, an additional advantage of the current procedure is that there is no need to compute any stress coefficients in calculating the element stress.

CPU time comparison for various 9-node plane elements is presented in Table 2. The present element (*AMF* plane) is more efficient than Lee & Rhiu's element. This is apparent in view of the different complexity for the stabilization matrices in En.(54) and Eqn.(61b).

methods of formulation	Lee et al's comparison [49]	Sze's et al's comparison [4]
displacement, 3x3 integration points	1.00	1.00

displacement, 2x2 integration points	0.53	0.44
hybrid strain formulation, see Eqn.(49)	1.95	- n.a. -
Lee & Rhiu's hybrid stabilization [49]	0.89	- n.a. -
AMF plane [4,55]	- n.a. -	0.62

Table 2 CPU time comparison for various 9-node plane elements

Fig.4 shows the popular cantilever problem for 9-node plane elements. The cantilever is subjected to a distributed end shear. The end deflection and the bending stress at the second order quadrature point B are computed. The results listed in Table 3 have been normalized by the analytical solutions given in the text of Timoshenko & Goodier [57]. All the advanced elements yield accurate predictions. The element "SQ9" [58] will be discussed in a later section.

		Mesh 1		Mesh 2		Mesh 3	
L/b	elements	deflect.	stress	deflect.	stress	deflect.	stress
10	displacement, 3x3	0.954	1.141	0.791	0.687	0.737	0.797
	displacement, 2x2	1.006	1.000	1.075	7.060	0.955	0.964
	hybrid strain [49]	0.990	1.000	0.975	0.914	0.960	0.923
	Lee & Rhiu [49]	0.995	1.022	1.014	1.085	0.986	0.981
	AMF plane [56]	0.991	1.000	1.019	0.908	0.941	0.919
	SQ9 [58]	0.991	- n.a. -	0.920	- n.a. -	0.955	- n.a. -
20	displacement, 3x3	0.939	0.193	0.758	0.679	0.441	0.501
	displacement, 2x2	1.002	1.000	1.071	1.060	0.951	0.964
	hybrid strain [49]	0.985	1.000	0.967	0.900	0.956	0.923
	Lee & Rhiu [49]	0.990	1.022	0.991	1.005	0.983	0.993
	AMF plane [56]	0.989	1.000	1.013	0.897	0.937	0.920
	SQ9 [58]	0.986	- n.a. -	1.013	- n.a. -	0.937	- n.a. -

Table 3 Normalized predictions for 9-node plane elements, see Fig.4

11.2 Twenty-Node Brick Element In this illustration, the more complicated 20-node brick is considered [59,60]. The displacement space of the element is generated by :

$$\left\{1,\ \xi,\ \eta,\ \zeta,\ \eta\zeta,\ \zeta\xi,\ \xi\eta,\ \xi^2,\ \eta^2,\ \zeta^2,\ \xi\eta\zeta,\ \eta\xi^2,\ \zeta\xi^2,\ \zeta\eta^2,\ \xi\eta^2,\ \xi\zeta^2,\ \eta\zeta^2,\ \eta\zeta\xi^2,\ \zeta\xi\eta^2,\ \xi\eta\zeta^2\right\}$$

(69a)

An alternative basis is :

$$\left\{1,\ \xi,\ \eta,\ \zeta,\ \eta\zeta,\ \zeta\xi,\ \xi\eta,\ \xi^2,\ \eta^2,\ \zeta^2,\ \xi\eta\zeta,\ \eta(3\xi^2-1),\ \zeta(3\xi^2-1),\ \zeta(3\eta^2-1),\ \xi(3\eta^2-1),\right.$$

$$\xi(3\zeta^2-1),\ \eta(3\zeta^2-1),\ \eta\zeta(3\xi^2-1),\ \zeta\xi(3\eta^2-1),\ \xi\eta(3\zeta^2-1)\Big\} \qquad (69b)$$

After some algebraic manipulations, six commutable mechanisms are identified :

$$\begin{Bmatrix} u_\xi \\ u_\eta \\ u_\varsigma \end{Bmatrix} = \begin{bmatrix} \xi(3\eta^2-1) & 0 & -\xi(3\zeta^2-1) & \zeta\xi(3\eta^2-1) & 0 & -\eta\xi(3\zeta^2-1) \\ -\eta(3\xi^2-1) & \eta(3\zeta^2-1) & 0 & -\zeta\eta(3\xi^2-1) & \xi\eta(3\zeta^2-1) & 0 \\ 0 & -\zeta(3\eta^2-1)0 & \zeta(3\xi^2-1) & 0 & -\xi\zeta(3\eta^2-1) & \eta\zeta(3\xi^2-1) \end{bmatrix} \begin{Bmatrix} \phi_1 \\ \vdots \\ \phi_6 \end{Bmatrix} \qquad (70)$$

where ϕ_i's are linear combinations of the nodal displacements. The derived covariant strain is :

$$\begin{bmatrix} \partial_\xi u_\xi & \partial_\eta u_\eta & \partial_\zeta u_\zeta & \partial_\zeta u_\eta + \partial_\eta u_\zeta & \partial_\xi u_\zeta + \partial_\zeta u_\xi & \partial_\eta u_\xi + \partial_\xi u_\eta \end{bmatrix}^T = \begin{bmatrix} \widehat{\mathbf{P}}_H \\ \mathbf{0}_{3\times 6} \end{bmatrix} \begin{Bmatrix} \phi_1 \\ \vdots \\ \phi_6 \end{Bmatrix} \qquad (71)$$

where

$$\widehat{\mathbf{P}}_H = \begin{bmatrix} (3\eta^2-1) & 0 & -(3\zeta^2-1) & \zeta(3\eta^2-1) & 0 & -\eta(3\zeta^2-1) \\ -(3\xi^2-1) & (3\zeta^2-1) & 0 & -\zeta(3\xi^2-1) & \xi(3\zeta^2-1) & 0 \\ 0 & -(3\eta^2-1) & (3\xi^2-1) & 0 & -\xi(3\eta^2-1) & \eta(3\xi^2-1) \end{bmatrix}$$

The mechanisms can be suppressed by the following contravariant stress :

$$\begin{bmatrix} \sigma_{\xi\xi} & \sigma_{\eta\eta} & \sigma_{\zeta\zeta} & \sigma_{\eta\zeta} & \sigma_{\zeta\xi} & \sigma_{\xi\eta} \end{bmatrix}_H^T = \begin{bmatrix} \widehat{\mathbf{P}}_H \\ \mathbf{0}_{3\times 6} \end{bmatrix} \boldsymbol{\beta}_H \qquad (72)$$

The shape function matrix for the assumed lower order Cartesian stress that constitutes an invertible $\overline{\mathbf{P}}$ is chosen to be :

$$\mathbf{P}_L = [\ \mathbf{I}_6 \quad \xi\mathbf{I}_6 \quad \eta\mathbf{I}_6 \quad \zeta\mathbf{I}_6 \quad \eta\zeta\mathbf{I}_6 \quad \zeta\xi\mathbf{I}_6 \quad \xi\eta\mathbf{I}_6 \quad \xi\eta\zeta\mathbf{I}_6\ ] \qquad (73)$$

The higher order Cartesian stress, which vanishes at the sub-integration points, is obtained from Eqn.(72) by using the constant contravariant stress transformation matrix evaluated at the element origin, i.e.

$$\begin{bmatrix} \sigma_{xx} & \sigma_{yy} & \sigma_{zz} & \sigma_{yz} & \sigma_{zx} & \sigma_{xy} \end{bmatrix}_H^T = \mathbf{P}_H \boldsymbol{\beta}_H = \frac{1}{J}\mathbf{T}_\sigma(\xi=\eta=\zeta=0) \begin{bmatrix} \widehat{\mathbf{P}}_H \\ \mathbf{0}_{3\times 6} \end{bmatrix} \boldsymbol{\beta}_H \qquad (74)$$

Again, the reciprocal of J is employed to yield the required orthogonality between $\mathbf{P}_L$ and $\mathbf{P}_H$. To form the higher order stiffness matrix, see Eqn.(61b), it is necessary to compute the inverse of the 6x6 matrix $\left\langle \mathbf{P}_H^T \mathbf{S} \mathbf{P}_H \right\rangle_H$. To reduce the computing time, the matrix is replaced by a diagonal $\mathbf{H}_{ll}$ [59,60]. CPU time ratio required to form displacement-based elements evaluated by the second order quadrature H20(8), the fourteen-point rule H20(14), the third order quadrature H20(27) and the present *hybrid stabilized element* is obtained [59,60] :

H20(8) : H20(14) : H20(27) : *hybrid stabilized* = 1.00 : 1.79 : 2.25 : 1.75 (75)

It is worth noting that the present element consumes less cpu time than H20(14). The relative accuracy for the 20-node elements are illustrated by the hemispherical shell problem depicted in Fig.5. Diametrical point loads of equal magnitude and alternating at 90^0 intervals are applied. Owing to its symmetry, only one quarter of the shell is modelled. Three NxN meshes are considered. Deflections at loaded point in the direction of the applied force are normalized by the reference solution of MacNeal & Harder [61] and listed in Table 4. Both the sub-integrated and the hybrid stabilized element are far better than the fully integrated elements.

mesh density	H20(8)	H20(14)	H20(27)	*hybrid stabilized* [59,60]
2 x 2	0.163	0.001	0.001	0.104
4 x 4	0.777	0.021	0.021	0.675
6 x 6	0.972	0.098	0.097	0.945

Table 4 Normalized deflections of 20-node elements in the hemispherical shell problem, see Fig.5

12. Explicit Hybrid Stabilization

For the two elements introduced in the last section, the employed contravariant stress transformation matrices are taken at the element origin and the orthogonality between $\mathbf{P}_L$ and $\mathbf{P}_H$ is strictly valid. In the 8-node brick element equipped with Allman's rotations [62-64], the true transformation matrix $\mathbf{T}_\sigma(\xi,\eta,\zeta)$ can be adopted without upsetting the patch test [65]. For the element, the lower order stress shape function is the same as the one given in Eqn.(73) and the commutable mechanisms are the same as the sub-integrated 20-node brick. In contrast to Eqn.(74), the higher order stress is chosen to be :

$$\boldsymbol{\sigma}_H = \left[\sigma_{xx} \quad \sigma_{yy} \quad \sigma_{zz} \quad \sigma_{yz} \quad \sigma_{zx} \quad \sigma_{xy} \right]_H^T = \mathbf{P}_H \boldsymbol{\beta}_H = \frac{1}{J} \mathbf{T}_\sigma(\xi,\eta,\zeta) \begin{bmatrix} \hat{\mathbf{P}}_H \\ \mathbf{0}_{3\times 6} \end{bmatrix} \boldsymbol{\beta}_H \qquad (76)$$

It can be checked that $\left\langle \mathbf{P}_L^T \mathbf{P}_H \right\rangle_H \neq \mathbf{0}$ but

$$\left\langle \mathbf{P}_H \right\rangle = \mathbf{0} \quad , \quad \left\langle \mathbf{P}_l^T \mathbf{P}_H \right\rangle_L = \left\langle \left[\xi \mathbf{I}_6 \quad \eta \mathbf{I}_6 \quad \zeta \mathbf{I}_6 \quad \eta\zeta \mathbf{I}_6 \quad \zeta\xi \mathbf{I}_6 \quad \xi\eta \mathbf{I}_6 \quad \eta\zeta\xi \mathbf{I}_6 \right]^T \mathbf{P}_H \right\rangle_L = \mathbf{0} \tag{77}$$

Hence, the effect of ignoring $\left\langle \mathbf{P}_l^T \mathbf{P}_H \right\rangle_H$ should be small. On the other hand, the displacement-derived strain can be expressed as :

$$\begin{aligned} \boldsymbol{\varepsilon}_q &= \left[\varepsilon_{xx}^u \quad \varepsilon_{yy}^u \quad \varepsilon_{zz}^u \quad 2\varepsilon_{yz}^u \quad 2\varepsilon_{zx}^u \quad 2\varepsilon_{xy}^u \right]^T = \mathbf{T}_\sigma^{-T} \left[\varepsilon_{\xi\xi}^u \quad \varepsilon_{\eta\eta}^u \quad \varepsilon_{\zeta\zeta}^u \quad 2\varepsilon_{\eta\zeta}^u \quad 2\varepsilon_{\zeta\xi}^u \quad 2\varepsilon_{\xi\eta}^u \right]^T \\ &= \mathbf{T}_\sigma^{-T} \left[\mathbf{x}_{,\xi}^T \mathbf{u}_{,\xi} \quad \mathbf{x}_{,\eta}^T \mathbf{u}_{,\eta} \quad \mathbf{x}_{,\zeta}^T \mathbf{u}_{,\zeta} \quad \mathbf{x}_{,\eta}^T \mathbf{u}_{,\zeta} + \mathbf{x}_{,\zeta}^T \mathbf{u}_{,\eta} \quad \mathbf{x}_{,\zeta}^T \mathbf{u}_{,\xi} + \mathbf{x}_{,\xi}^T \mathbf{u}_{,\zeta} \quad \mathbf{x}_{,\xi}^T \mathbf{u}_{,\eta} + \mathbf{x}_{,\eta}^T \mathbf{u}_{,\xi} \right]^T \end{aligned} \tag{78}$$

where

$$\mathbf{u} = [\, u \quad v \quad w \,]^{\mathrm{T}} \quad , \quad \mathbf{x} = [\, x \quad y \quad z \,]^{\mathrm{T}}$$

are the displacement and position vectors, respectively. From Eqn.(76) and Eqn.(78),

$$\boldsymbol{\beta}_H^T \left\langle \mathbf{P}_H^T \mathbf{B}_q \right\rangle \mathbf{q} = \left\langle \boldsymbol{\sigma}_H^T \boldsymbol{\varepsilon}_q \right\rangle = \boldsymbol{\beta}_H^T \int_{-1}^{+1}\int_{-1}^{+1}\int_{-1}^{+1} \left[\begin{array}{c:c:c} \begin{array}{c} (3\eta^2-1)x_{,\xi}\,\partial_\xi - (3\xi^2-1)x_{,\eta}\,\partial_\eta \\ (3\zeta^2-1)x_{,\eta}\,\partial_\eta - (3\eta^2-1)x_{,\zeta}\,\partial_\zeta \\ (3\xi^2-1)x_{,\zeta}\,\partial_\zeta - (3\zeta^2-1)x_{,\xi}\,\partial_\xi \\ \zeta(3\eta^2-1)x_{,\xi}\,\partial_\xi - \zeta(3\xi^2-1)x_{,\eta}\,\partial_\eta \\ \xi(3\zeta^2-1)x_{,\eta}\,\partial_\eta - \xi(3\eta^2-1)x_{,\zeta}\,\partial_\zeta \\ \eta(3\xi^2-1)x_{,\zeta}\,\partial_\zeta - \eta(3\zeta^2-1)x_{,\xi}\,\partial_\xi \end{array} & \begin{array}{c} (3\eta^2-1)y_{,\xi}\,\partial_\xi - (3\xi^2-1)y_{,\eta}\,\partial_\eta \\ (3\zeta^2-1)y_{,\eta}\,\partial_\eta - (3\eta^2-1)y_{,\zeta}\,\partial_\zeta \\ (3\xi^2-1)y_{,\zeta}\,\partial_\zeta - (3\zeta^2-1)y_{,\xi}\,\partial_\xi \\ \zeta(3\eta^2-1)y_{,\xi}\,\partial_\xi - \zeta(3\xi^2-1)y_{,\eta}\,\partial_\eta \\ \xi(3\zeta^2-1)y_{,\eta}\,\partial_\eta - \xi(3\eta^2-1)y_{,\zeta}\,\partial_\zeta \\ \eta(3\xi^2-1)y_{,\zeta}\,\partial_\zeta - \eta(3\zeta^2-1)y_{,\xi}\,\partial_\xi \end{array} & \begin{array}{c} (3\eta^2-1)z_{,\xi}\,\partial_\xi - (3\xi^2-1)z_{,\eta}\,\partial_\eta \\ (3\zeta^2-1)z_{,\eta}\,\partial_\eta - (3\eta^2-1)z_{,\zeta}\,\partial_\zeta \\ (3\xi^2-1)z_{,\zeta}\,\partial_\zeta - (3\zeta^2-1)z_{,\xi}\,\partial_\xi \\ \zeta(3\eta^2-1)z_{,\xi}\,\partial_\xi - \zeta(3\xi^2-1)z_{,\eta}\,\partial_\eta \\ \xi(3\zeta^2-1)z_{,\eta}\,\partial_\eta - \xi(3\eta^2-1)z_{,\zeta}\,\partial_\zeta \\ \eta(3\xi^2-1)z_{,\zeta}\,\partial_\zeta - \eta(3\zeta^2-1)z_{,\xi}\,\partial_\xi \end{array} \end{array} \right] \left\{ \begin{array}{c} u \\ v \\ w \end{array} \right\} d\xi\, d\eta\, d\zeta \tag{79}$$

The stabilization vectors presented as the row vectors in $\left\langle \mathbf{P}_H^T \mathbf{B}_q \right\rangle$ turn out to be some very simple expressions of the nodal coordinates and can be programmed explicitly instead of resorting to numerical integration loops. Moreover,

$$\left\langle \mathbf{P}_H^T \mathbf{S} \mathbf{P}_H \right\rangle_H = \int_{-1}^{+1}\int_{-1}^{+1}\int_{-1}^{+1} \frac{1}{J} \begin{bmatrix} \widehat{\mathbf{P}}_H \\ \mathbf{0}_{3\times 6} \end{bmatrix}^T \mathbf{T}_\sigma^T \mathbf{S} \mathbf{T}_\sigma \begin{bmatrix} \widehat{\mathbf{P}}_H \\ \mathbf{0}_{3\times 6} \end{bmatrix} d\xi d\eta d\zeta \tag{80}$$

After J and $\mathbf{T}_\sigma(\xi,\eta,\zeta)$ are, respectively, replaced by $J_o = J(\xi=\eta=\zeta=0)$ and $[\ \mathbf{T}_1 \quad \mathbf{T}_2 \quad \mathbf{T}_3 \quad \mathbf{T}_4 \quad \mathbf{T}_5 \quad \mathbf{T}_6\ ] = \mathbf{T}_\sigma(\xi=\eta=\zeta=0)$, the resulting admissible version of $\left\langle \mathbf{P}_H^T \mathbf{S} \mathbf{P}_H \right\rangle_H$ is :

$$\mathbf{H}_{HH} = \frac{1}{J_o}\int_{-1}^{+1}\int_{-1}^{+1}\int_{-1}^{+1} \widehat{\mathbf{P}}_H^T \widehat{\mathbf{S}} \widehat{\mathbf{P}}_H \, d\xi d\eta d\zeta$$

$$= \frac{32}{15 J_o} \times diag. \left\{ \begin{bmatrix} \widehat{S}_{11}+\widehat{S}_{22} & -\widehat{S}_{13} & -\widehat{S}_{23} \\ & \widehat{S}_{22}+\widehat{S}_{33} & -\widehat{S}_{21} \\ sym. & & \widehat{S}_{33}+\widehat{S}_{11} \end{bmatrix} \quad \widehat{S}_{11}+\widehat{S}_{22} \quad \widehat{S}_{22}+\widehat{S}_{33} \quad \widehat{S}_{33}+\widehat{S}_{11} \right\} \tag{81}$$

where

$$\widehat{\mathbf{S}} = [\widehat{S}_{ij}] = \begin{bmatrix} \mathbf{T}_1 & \mathbf{T}_2 & \mathbf{T}_3 & \mathbf{0}_{6\times 3} \end{bmatrix}^T \mathbf{S} \begin{bmatrix} \mathbf{T}_1 & \mathbf{T}_2 & \mathbf{T}_3 & \mathbf{0}_{6\times 3} \end{bmatrix}$$

Unlike the previous *hybrid stabilization*, higher order integration rule needs not be used in programming the *explicit hybrid stabilization vectors*. This further enhances the computational efficiency of the elements.

The two-element cantilever problem shown in Fig.6 is examined. Point moments are applied to the four end nodes. The average end deflections and the bending stresses at point B, the centre of the element face, are computed and normalized by the analytical solutions [57]. The results with varying degree of mesh distortion (characterized by "e") are shown in Fig.7. HEX8RX is the *STIF73* element in the commercial finite element code *ANSYS* [63]. Displacement of the "present element" are supplemented with the following bubble (internal) displacement d.o.f.s [65] :

$$\mathbf{u}_\lambda = (1-\xi^2)(1-\eta^2)(1-\zeta^2)\ \mathbf{I}_3 \begin{Bmatrix} \lambda_1 \\ \lambda_2 \\ \lambda_3 \end{Bmatrix} \tag{82}$$

for enforcing the homogenous equilibrium condition in the assumed stress [66]. Meanwhile, three incompatible displacement modes are employed in HEX8RX. Mechanisms of HEX8RX are suppressed by generalizing MacNeal's perturbation stabilization schemes [67]. Despite of the employed small perturbation parameter, HEX8RX is more susceptible to mesh distortion.

13. Closure

In this paper, the evolution of *AMF* has been reviewed. Several sample elements are used to illustrate how the technique can be applied to lower and higher order elements with and without internal displacement d.o.f.s. Although only *AMF* hybrid stress elements are discussed, the technique can readily be extended to hybrid strain elements which are sometimes deemed to be more suitable for nonlinear analysis. Besides the *AMF* elements presented in references [14,16,42-45,47,55,58-60,64,65], there still remains a large number of practical element configurations that *AMF* can be applied.

Explicit hybrid stabilization vectors have also been derived for the 9-node Lagrangian shell element [58]. The explicit form of the vectors are given in reference [68]. The element, designated as SQ9, passes the patch test only if the mesh are sub-parametric (the element central node locates at the parametric origin defined by the four corner nodes and the edge nodes are mid-edge nodes). This is because $\langle \mathbf{P}_H \rangle_H$ equals zero only when the element is sub-parametric despite of the general vanishing nature of $\langle \mathbf{P}_H \rangle_L$. The predictions of SQ9 for the benchmark test depicted in Fig.4 have been listed in Table 3.

As a matter of fact, if one sticks to sub-parametric elements, *explicit stabilization vectors* can also be derived for the 20-node brick expounded in Section 11.2 and many other higher order elements. It should be remarked that the so-derived *explicit stabilization vectors* can still suppress the mechanisms but will slightly destroy the element consistency. Whether the users would accept sub-parametric elements or not depends very much on their finite element know-how. In the recent text of MacNeal [69], he mentioned that a sub-parametrically formulated 6-node membrane element once available in MSC/NASTRAN was not popular with users. It was probably because most users well perceive the geometric discretization error but remain relatively unaware of the substantial drop in element accuracy when the element ediges are curved (illustrations can be found in reference [70,71]). Nevertheless, we know that most 6-node and 9-node shell elements only pass the plate bending patch test when the elements are sub-parametric and they have been being used in many commercial codes for decades.

Since every mesh becomes practically sub-parametric after successive refinement, stabilization vectors with sub-parametric consistency should be acceptable. For all the examined curved shell problems reported in reference [58], SQ9 yields close predictions to, if not more accurate than, the γ–ϕ stabilized element [54] which passes the plate bending patch test even if the mesh is not sub-parametric. Moreover, there exist a large number of elements (especially, plate/shell elements) in the open literature that only exhibit sub-parametric consistency. Except for curved shells, only a very small portion of the elements in finite element meshes for infinitesimal strain problems are not sub-parametric. For large deformation analyses, the distorted edges are often straightened in the remeshing process so as to maintain the element accuracy, see e.g. reference [71]. Of course, further investigations should be carried out to compare the relative efficiency and accuracy of the stabilization vectors which are strictly consistent and the stabilization vectors which are only sub-parametric consistent.

References

1. T.H.H.Pian, "Derivation of element stiffness matrices by assumed stress distributions", *AIAA J.*, **2**, 1333-1336 (1964)

2. T.H.H.Pian, "Thirty-year history of hybrid stress finite element methods", *Proc.Y.K.Cheung Symposium*, pp.23-31, P.K.K.Lee & L.G.Tham (eds.), Dept. of Civil & Struct. Engrg., the University of Hong Kong, 1994

3. T.H.H.Pian, S.W.Lee, Notes of finite elements for nearly incompressible materials, *AIAA J.*, **14**, 824-826 (1976)

4. K.Y.Sze, H.Fan, C.L.Chow, "Elimination of spurious kinematic and pressure modes in biquadratic plane element", *Inter.J.Numer.Methods Engrg.*, accepted for publication

5. H.-S.Jing, M.-L.Liao, "Partial hybrid stress element for the analysis of thick laminated composite plates", *Inter.J.Numer.Methods Engrg.*, **28**, 2813-2827 (1989)

6. T.H.H.Pian, M.-S.Li, "Stress analysis of laminated composites by hybrid finite elements", in *Discretization Methods in Structural Mechanics*, G.Kuhn & H.Mang (eds.), Springer-Verlag, Berlin, 1989

7. J.Zhang, N.Katsube, "A hybrid finite element method for heterogeneous materials with randomly dispersed elastic inclusions", *Finite Elements in Analysis & Design*, **19**, 45-55 (1995)

8. R.L.Spilker, S.M.Maskeri, E.Kania, "Plane isoparametric hybrid-stress elements: invariance and optimal sampling", *Inter.J.Numer.Methods Engrg.*, **17**, 1469-1496 (1981)

9. K.Y.Sze, C.L.Chow, W.-J.Chen, "On invariance of isoparametric hybrid elements", *Commun. Appl.Numer.Methods*, **8**, 385-406 (1992)

10. B.M.Irons, "The semi-loof shell element", in *Finite Elements for Thin Shells and Curved Members*, Chap.11, pp.197-222 , D.G.Ashwell & R.H.Gallagher (eds), John Wiley & Sons, New York, 1976

11. T.H.H.Pian, K.Sumihara, "Hybrid semiloof elements for plates and shells upon a modified Hu-Washizu Principles", *Computers & Structures*, **19**, 165-173 (1984)

12. K.Y.Sze, "Minimal assumed moments and optimal local coordinates for plate elements based upon the complementary energy functional", *Computational Mechanics*, **14**, 586-595 (1994)

13. W-J.Chen, C.L.Chow, K.Y.Sze, "An orthogonal approach for hybrid element methods", unpublished manuscript, submitted for publication in November 1989

14. K.Y.Sze, C.L.Chow, "Efficient hybrid/mixed element formulations by free formulation and energy orthogonality", *Proc.1st Int.Conf. of Computer Aided Assessment and Control of Localized Damage 1990 : Vol.3 - Advanced Computational Methods*, pp.143-156, ed. M.H. Aliabadi, C.A.Brebbia & D.J.Cartwright, Springer-Verlag, 1990

15. Y.K.Cheung, W.-J.Chen, "Refined hybrid method for plane isoparametric element using an orthogonal approach", *Computers & Structures*, **42**, 683-694 (1992)

16. K.Y.Sze, C.L.Chow, "Efficient hybrid/mixed elements using admissible matrix formulation", *Computer Methods Appl.Mech.Engrg.*, **99**, 1-26 (1992)

17. W-J.Chen, Y.K.Cheung, "Three-dimensional 8-node and 20-node refined hybrid isoparametric elements", *Inter.J.Numer.Methods Engrg.*, **35**, 1871-1889 (1992)

18. T.H.H.Pian, D.-P.Chen, "Alternative ways for formulation of hybrid stress elements", *Inter.J.Numer. Methods Engrg.*, **18**, 1679-1684 (1982)

19. T.H.H.Pian, K.Sumihara, "Rational approach for assumed stress finite elements", *Inter.J. Numer.Methods Engrg.*, **20**, 1685-1695 (1984)

20. T.H.H.Pian, P.Tong, "Relations between incompatible displacement model and hybrid stress model", *Inter.J.Numer.Methods Engrg.*, **22**, 173-181 (1986)

21. W.-J.Chen, Y.K.Cheung, "A new approach for the hybrid element method", *Inter.J.Numer. Methods Engrg.*, **24**, 1697-1709 (1987)

22. W.-J.Chen, Y.K.Cheung, "Axisymmetric solids elements by the generalized hybrid method", *Computers & Structures*, **27**, 745-752 (1987)

23. P.G.Bergan, L.Hanssen, "A new approach for deriving 'good' element stiffness matrices", in *The Mathematics of Finite Elements and Applications, Vol.II*, pp.483-497, J.R.Whiteman (ed.), Academic Press, London, 1976

24. P.G.Bergan, "Finite elements based on energy orthogonal functions", *Inter.J.Numer.Methods. Engrg.*, **15**, 1541-1555 (1980)

25. C.A.Felippa, "Parametrized multifield variational principles in elasticity : II.hybrid functionals and the free formulation", *Comm.Appl.Numer.Meth.*, **5**, 89-98 (1989)

26. R.L.Taylor, J.C.Simo, O.C.Zienkiewicz, C.H.Chan, "The patch test - a condition for assessing fem convergence", *Inter.J.Numer.Methods Engineering*, **22**, 39-62 (1986)

27. C.Militello, C.A.Felippa, "The individual element test revisited", in *The Finite Elements in the 90"s - a book dedicated to O.C.Zienkiewicz*, pp.554-564, E. Oñate , J.Periaux and A. Samuelsson (eds.), Springer-Verlag, Barcelona, 1991

28. T.J.R.Hughes, T.E.Tezduyar, "Finite elements based upon Mindlin Plate theory with particular reference to the four-node bilinear isoparametric element", *J.Appl.Mech.*, **48**, 587-596 (1981)

29. R.H.MacNeal, "Derivation of element stiffness matrices by assumed strain distributions", *Nuclear Engrg. & Design*, **70**, 3-12 (1982)

30. K.-J.Bathe, E.N.Dvorkin, "A four-node plate bending element based on Mindlin/Reissner plate theory and a mixed interpolation", *Inter.J.Numer.Methods Engrg.*, **21**, 367-383 (1985)

31. J.C.Simo, T.J.R.Hughes, "On the variational foundations of assumed strain methods", *J.Appl. Mech.*, **53**, 51-54 (1986)

32. J.C.Simo, M.S.Rifai, "A class of mixed assumed strain methods and the method of incompatible modes", *Inter.J.Numer.Methods Engrg*., **29**, 1595-1638 (1990)

33. G.Strang, G.J.Fix, *Analysis of the Finite Element Method*, Prentice-Hall, New Jersey, 1973

34. R.L.Taylor, P.J.Beresford, E.L.Wilson, "A non-conforming element for stress analysis", *Inter.J. Numer.Methods Engrg.*, **10**, 1211-1219 (1976)

35. C.-C.Wu, M.-G.Huang, T.H.H.Pian, "Consistency condition and convergence criteria of incompatible elements: general formulation of incompatible functions and its application", *Computers & Structures*, **27**, 639-644 (1987)

36. K.Y.Sze, C.L.Chow, "An incompatible element for axisymmetric structure and its modification by hybrid method", *Inter.J.Numer.Methods Engrg.*, **31**, 385-405 (1991)

37. C.A.Felippa, P.G.Bergan, "A triangular element based on an energy-orthogonal free formulation", *Computer Methods Appl.Mech.Engrg*., **61**, 129-160 (1987)

38. C.Militello, C.A.Felippa, "The first ANDES elements : 9-DOF plate bending triangles", *Computer Methods Appl.Mech.Engrg*., **93**, 217-246 (1991)

39. K.Y.Sze, `Derivation of accuracy and efficient elements by mixed method and free formulation', *Proc. 1st U.S. National Congress on Computational Mechanics*, Chicago, July 1991

40. I. Babuška , "The finite element method with Lagrangian multipliers", Num.Math., **20**, 179-192 (1973)

41. W.-M.Xue, L.Z.Karlovitz, S.N.Atluri, "On the existence and stability conditions for mixed-hybrid finite element solutions based on Reissners Variational Principle", *Inter.J.Solid & Structures*, **21**, 97-116 (1985)

42. K.Y.Sze, "Efficient formulation of robust hybrid elements using orthogonal stress/strain interpolants and admissible matrix formulation, *Inter.J.Numer.Methods Engrg.*, **35**, 1-20 (1992)

43. K.Y.Sze, H.Fan, `An Economical Assumed stress Brick Element and Its Implementation', *Finite Elements in Analysis & Design*, accepted

44. K.Y.Sze, A.Ghali, `A two-field solid element suiting thin-mesh analysis by admissible matrix formulation', *Engineering Computations*, **9**, 649-668 (1992)

45. K.Y.Sze, A.Ghali, "An hexahedral element for plates, shells and beams by selective scaling", *Inter.J.Numer. Methods Engrg.*, **36**, 1519-1540 (1993)

46. S.P.Timoshenko, S.Woinowsky-Krieger, *Theory of Plates and Shells*, McGraw-Hill, New York, 1970

47. K.Y.Sze, C.L.Chow, "A mixed formulation of 4-node Mindlin/Reissner shell/plate element with interpolated transverse shear strains", *Computers & Structures*, **40**, 775-784 (1991)

48. J.J.Rhiu, S.W.Lee, "A new mixed formulation for finite element analysis of thin shell structures, in *Hybrid and Mixed Finite Element Methods*, ASME AMD-Vol.73, pp.25-38, R.L.Spilker & K.W.Reed (eds.), 1985

49. S.W.Lee, J.J.Rhiu, "A new efficient approach to the formulation of mixed finite element models for structural analysis", *Inter.J.Numer.Methods Engrg.*, **21**, 1629-1641 (1986)

50. M.F.Ausserer, S.W.Lee, "An eighteen-node solid element for thin shell analysis", *Inter.J.Numer. Methods Engrg.*, **26**, 1345-1364 (1988)

51. J.J.Rhiu, R.M.Russell, S.W.Lee, "Two higher-order shell finite elements with stabilization matrix", *AIAA J.*, **28**, 1517-1524 (1990)

52. T.Belytschko, W.K.Liu, J.J.-S.Ong, "Mixed variational principles and stabilization of spurious modes in the 9-node element", *Computer Methods Appl.Mech.Engrg.*, **62**, 275-292 (1987)

53. W.K.Liu, J.S-.J.Ong, R.A.Uras, "Finite element stabilization matrices - a unification approach", *Computer Methods Appl.Mech.Engrg.*, **53**, 13-46 (1985)

54. T.Belytschko, B.K.Wong, "Assumed strain stabilization procedure for the 9-node Lagrange shell element", *Inter.J.Numer.Methods.Engrg.*, **28**, 385-414 (1989)

55. K.Y.Sze, "A novel approach for devising higher order hybrid elements", *Inter.J.Numer.Methods Engrg.*, **36**, 3303-3316 (1993)

56. D.S.Malkus, T.J.R.Hughes, "Mixed finite element methods - reduced and selective integration techniques : a unification of concepts", *Computer Methods Appl.Mech.Engrg.*, **15**, 63-81 (1978)

57. S.P.Timoshenko, J.N.Goodier, *Theory of Elasticity*, McGraw-Hill, New York, 1982

58. K.Y.Sze, "An explicit hybrid-stabilized 9-node Lagrangian shell element", *Computer Methods Appl.Mech.Engrg.*, **117**, 361-379 (1994)

59. K.Y.Sze, "Control of spurious mechanisms for 20-node and transition sub-integrated hexahedral elements", *Inter.J.Numer.Methods Engrg.*, **37**, 2235-2250 (1994)

60. K.Y.Sze, "Stabilization schemes for 12-node to 21-node brick elements based on orthogonal and consistently assumed stress modes", *Computer Methods App.Mech.Engrg.*, **119**, 325-340 (1994)

61. R.H.MacNeal, R.L.Harder, "A proposed standard set of problems to test finite element accuracy", *Finite Elements in Analysis & Design*, **1**, 3-20 (1985)

62. D.J.Allman, "A compatible triangular element including vertex rotations for plane elasticity analysis", *Computers & Structures*, **19**, 1-8 (1984)

63. S.M.Yunus, T.P.Pawlak, "Solid elements with rotational degrees of freedom : part I - hexahedron elements", *Inter.J.Numer.Methods Engrg.*, **31**, 573-592 (1991)

64. K.Y.Sze, A.Ghali, "A hybrid brick element with rotational d.o.f.", *Computational Mechanics*, **12**, 147-163 (1993)

65. K.Y.Sze, Y.S.Sim, A.K.Soh, "Explicit hybrid-stabilized solid elements with rotational degrees of freedom", in preparation

66. T.H.H.Pian, D.-P.Chen, "Alternative ways for formulation of hybrid stress elements", *Inter.J. Numer.Methods Engrg*., **18**, 1679-1684 (1982)

67. R.H.MacNeal, R.L.Harder, "A refined four-noded membrane element with rotational degrees of freedom", *Computers & Structures*, **28**, 75-84 (1989)

68. K.Y.Sze, "Assumed stress stabilization vectors for 9-node shell element", *Proc.Inter.Conf.on Computational Engineering Science*, Hawaii, July/August, 1995, accepted

69. R.H.MacNeal, *Finite Elements : Their Design and Performance*, Marcel Dekker, New York, 1994

70. N.-S.Lee, K.-J.Bathe, "Effects of element distortions on the performance of isoparametric elements", *Inter.J.Numer.Methods Engrg.*, **36**, 3553-3576 (1993)

71. N.-S.Lee, K.-J.Bathe, "Error indicators and adaptive remeshing in large deformation finite element anlaysis", *Finite Elements in Analysis & Design*, **16**, 99-139 (1994)

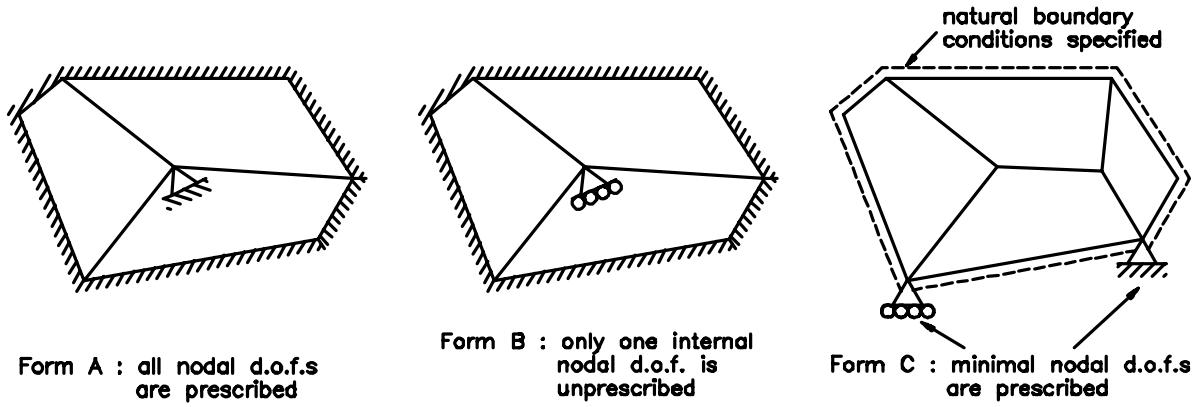

Fig.1 Graphical descriptions of Form A, Form B and Form C Tests

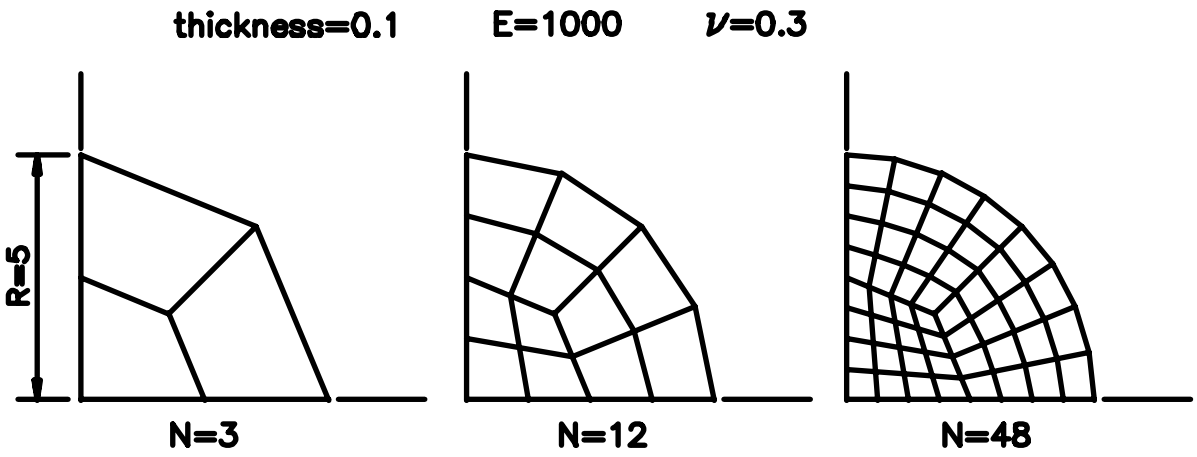

Fig.2 Meshes for clamped circular plate

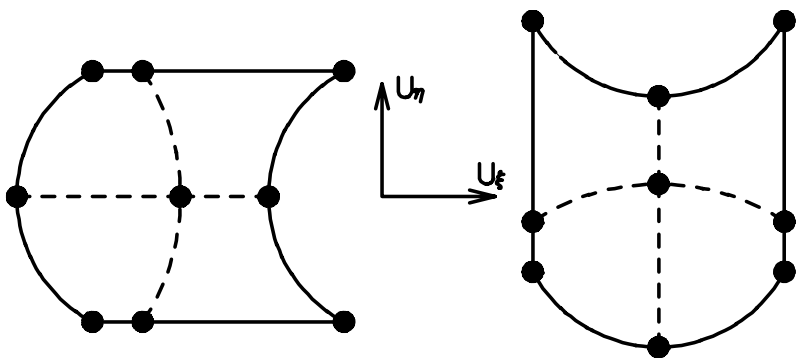

Fig.3 Commutable mechanisms of nine-node membrane elements

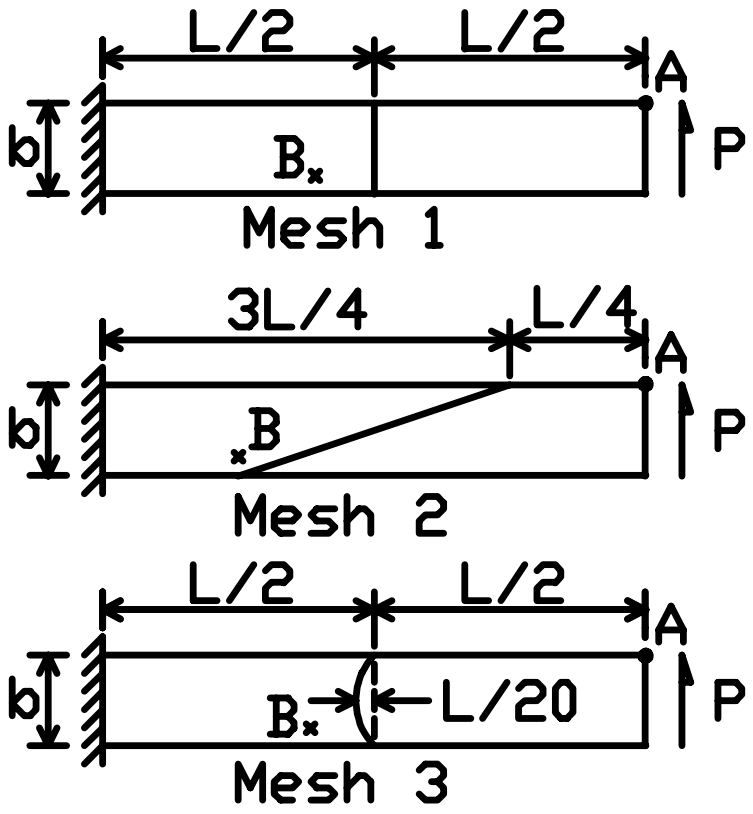

Fig.4 Cantilever tests for 9-node elements, Poisson's ratio equal to 0.3

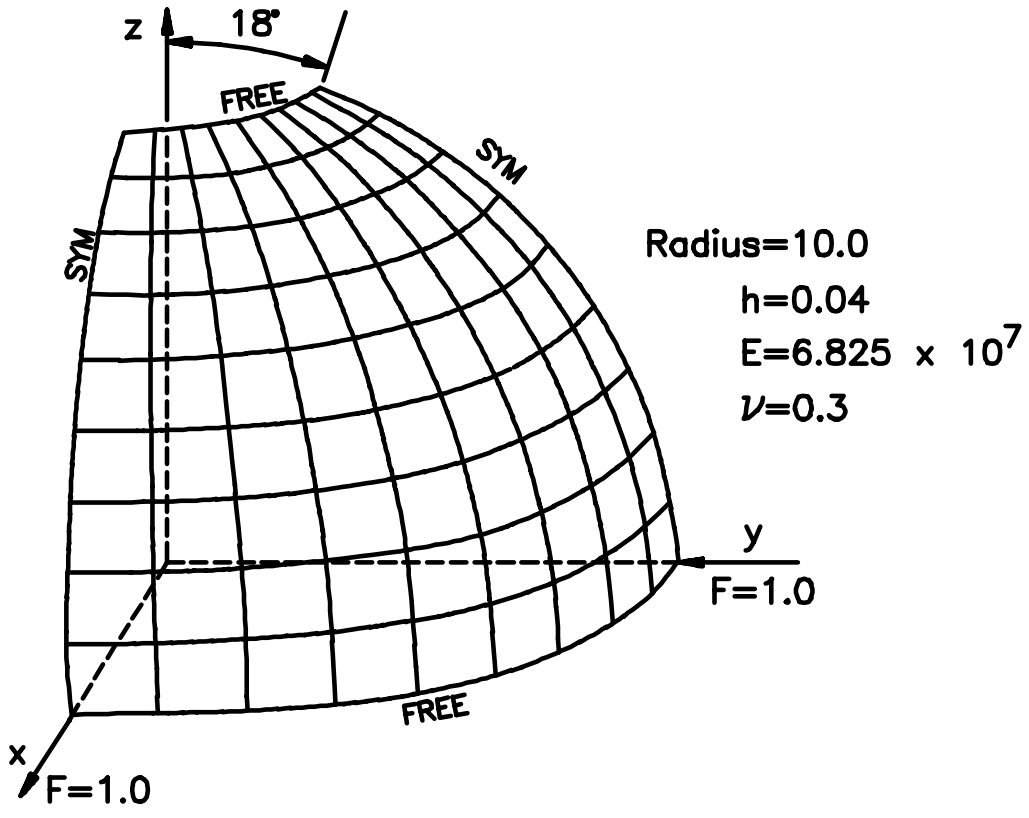

Fig.5 Hemispherical shell problem, for 20-node brick elements

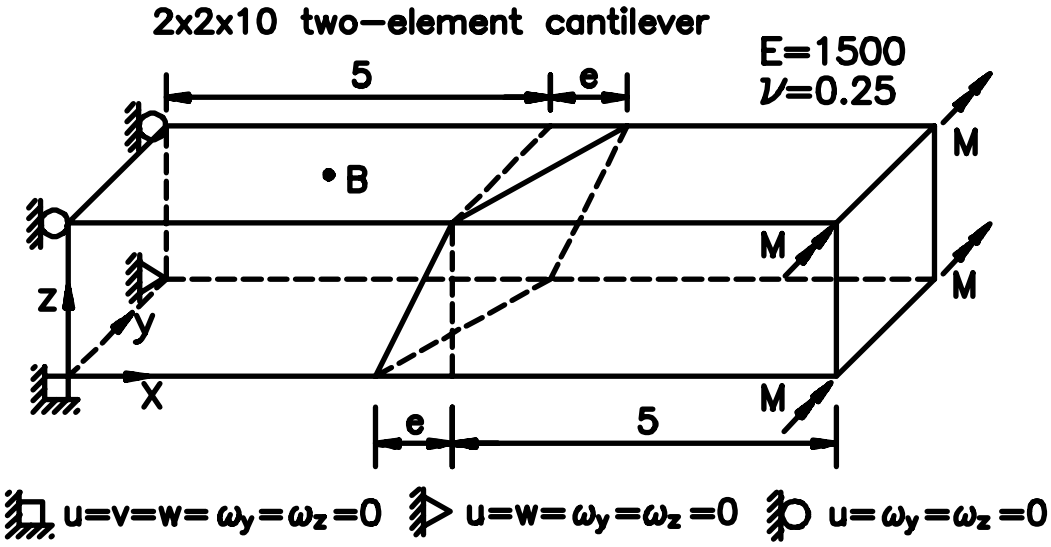

Fig.6 Two-element cantilever problem for 8-node bricks with rotational degrees of freedom and three bubble displacement modes

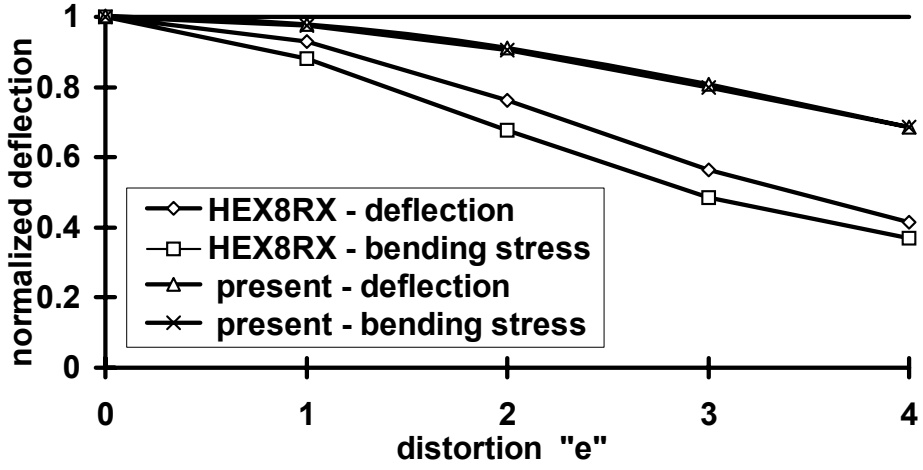

Fig.7 Normalized end defections and bending stresses at point B, see Fig.6 for 8-node elements with rotational d.o.f.s